Measurement report: Soil reactive nitrogen gas emissions in the Tibetan Plateau

Lingling Deng[1,#], Yuhan Chen[1,#], Chunxiang Ye[2], Rui Wang[1], Ruhai Wang[3], Zehua Fu[3], Hongfang Zhao[1,*], Dianming Wu[1,*]

[1]Key Laboratory of Geographic Information Science (Ministry of Education), School of Geographic Sciences, East China Normal University, 200241 Shanghai, China
[2]State Key Joint Laboratory for Environmental Simulation and Pollution Control, Center for Environment and Health, College of Environmental Sciences and Engineering, Peking University, Beijing 100871, P. R. China
[3]State Key Laboratory of Soil and Sustainable Agriculture, Institute of soil Sciences, Chinese Academy of Sciences, 210008 Nanjing, China
[#]Lingling Deng and Yuhan Chen contributed equally to this work.

Correspondence to: Dianming Wu (dmwu@geo.ecnu.edu.cn), Hongfang Zhao (hfzhao@geo.ecnu.edu.cn)

Abstract. The Tibetan Plateau, highly sensitive to climate change, exerts strong atmospheric oxidation capacity partly through rapid cycling of atmospheric reactive nitrogen (Nr). Soil Nr emissions play a crucial role in atmospheric nitrogen cycling and oxidation capacity, yet their emissions on the Tibetan Plateau remain poorly quantified. Combining dynamic chamber measurements, laboratory analysis, and a parameterized model, we assessed the characteristics, driving factors, spatial distribution and annual emissions of soil Nr in the Tibetan Plateau. We found that the optimum soil fluxes of nitrous acid (HONO), nitric oxide (NO), nitrogen dioxide (NO_2), and ammonia (NH_3) were 21.6 ± 8.4, 43.7 ± 14.7, 15.8 ± 1.3, and 190.0 ± 116.3 ng N m^{-2} s^{-1}, respectively. These emissions were mainly influenced by soil pH, nutrient content, and microbial community composition. After exposure to atmospheric NO_x and ozone (O_3), Nr emissions from forest soils were enhanced but those from croplands and grasslands were suppressed. The estimated annual emissions of soil HONO, NO, and NO_x from Tibetan Plateau to be 7.0 ± 3.4 Gg N yr^{-1}, 11.6 ± 7.8 Gg N yr^{-1}, and 20.3 ± 7.0 Gg N yr^{-1}, respectively. Soil HONO emissions contribute approximately 10.5% of the external (NO_x-independent) daytime atmospheric HONO sources and modulate the regional atmospheric chemical balance by elevating the HONO/NO_x ratio. Our results provide the first integrated quantification of soil Nr emissions on the Tibetan Plateau and emphasize their importance for regional nitrogen cycling and atmospheric oxidation capacity.

1 Introduction

Soil reactive nitrogen (Nr) gas emissions play a key role in the global nitrogen cycle, climate warming and atmospheric chemistry. Nr such as nitrous acid (HONO), nitrogen oxides [NO_x, including nitric oxide (NO) and nitrogen dioxide (NO_2)], and ammonia (NH_3), are capable of directly influencing key atmospheric processes related to climate and air quality (McCalley et al., 2011; Sutton et al., 2009). For example, HONO and NO_x regulate the formation of hydroxyl radicals (OH·) and accelerate

gas-phase chemical reactions, leading to tropospheric O_3 formation and bursts of secondary aerosols [e.g., nitrate, sulphate, and secondary organic aerosols (SOA)] (Behrendt et al., 2014; Delaria and Cohen, 2023; Hereid and Monson, 2001; Liu et al., 2021; Sörgel et al., 2015). NH_3 promotes aerosol and cloud formation, affecting radiative attenuation and causing cooling of the Earth's surface (Behera et al., 2013; Bray et al., 2021; Erisman et al., 2011; McCalley et al., 2011). Given the diverse climatic and atmospheric effects of individual Nr species, (Liu et al., 2019; Ma et al., 2022; Song et al., 2023; Wu et al., 2022a), isolating the components of Nr and thoroughly understanding the specific contributions from soil sources is essential for accurately assessing their environmental impacts and informing effective mitigation strategies.

Soils release Nr via a series of biotic and abiotic processes, mainly through microbial nitrification and denitrification, and chemical acid-base equilibrium (Bhattarai et al., 2021; Ermel et al., 2018; Heil et al., 2016; Hong et al., 2025; Kumar et al., 2025; Medinets et al., 2015; Mushinski et al., 2019; Oswald et al., 2013; Su et al., 2011; VandenBoer et al., 2015; Wu et al., 2019). Upon comparing Nr emission from sterilized and natural soils, it was found that the emissions of HONO and NO from sterilized soils were significantly reduced (Oswald et al., 2013; Wu et al., 2019). It was also demonstrated that microbial processes contribute 8-42 times more to HONO emissions from agricultural soils than abiotic processes (Bhattarai et al., 2021). Therefore, the activity of soil N cycling microorganisms can dominate the rate and total amount of Nr emission (Maier et al., 2022). Furthermore, Nr is modulated by soil environmental factors, such as soil acidity, moisture, temperature, nitrogen fertilizer application, vegetation cover, inorganic nitrogen content (NO_3^-, NO_2^-, and NH_4^+), soil texture, carbon/nitrogen (C/N) ratio, mineralization and (de)nitrification rates (Behrendt et al., 2014; Bhattarai et al., 2018; Delaria and Cohen, 2023; Donaldson et al., 2014; Kim and Or, 2019; Maljanen et al., 2013; Pilegaard, 2013; Su et al., 2013; VandenBoer et al., 2015). Agricultural activities, particularly the application of nitrogen fertilizers, have been shown to significantly enhance the emissions of HONO, NO, and NH_3 from soils and contribute to nitrate leaching to groundwater/aquifers, a major environmental concern exhibiting substantial spatial and crop-specific variability (Ren et al., 2025; Wang et al., 2025b). Results showed that NO and NH_3 emissions from agricultural fertilized soils can account for 15% and 23% of the total global agricultural Nr emissions, respectively (Lu et al., 2021; Ma et al., 2022; Tian et al., 2023). Agricultural soils are also a hotspot for HONO emissions (Wu et al., 2022b). However, the pattern of soil Nr emissions, particularly for HONO, remains unclear on the Tibetan Plateau.

The Tibetan Plateau promotes sustained atmospheric oxidation capacity due to strong ultraviolet radiation, high O_3 and water vapor concentrations, and rapid circulation of atmospheric Nr (Chen et al., 2022b; Liang et al., 2021; Tang et al., 2023). Several investigations have reported that O_3 concentrations at the surface of the Tibetan Plateau range from 25 to 100 ppb, and tend to be higher in spring and winter (Li et al., 2022; Škerlak et al., 2014; Xu et al., 2023; Xu et al., 2018; Yin et al., 2017). Moreover, external cycling (NO_x-independent) of Nr has been observed in the Tibetan Plateau region, triggering elevated HONO and NO_x concentrations and strengthening the local atmospheric oxidizing capacity (Wang et al., 2023a). Global warming and human activities also accelerated natural and anthropogenic emissions of NO_x in the Tibetan Plateau region, probably elevating O_3 concentrations further in the background region (Lyu et al., 2023; Xu et al., 2023).

删除了：Recently, it was demonstrated that lakes on the Tibetan Plateau were NO_x emission hotspots, equivalent to the anthropogenic emissions of numerous megacities, with an average emission intensity of 63.4 μg N m^{-2} h^{-1}, which exceeded the NO_x emission intensity from crop fields (Kong et al., 2023).

In this work, we combined dynamic chamber flux measurement, laboratory analysis, and a parameterized model to assess the characteristics, driving factors, spatial distribution and annual emissions of soil Nr in Tibet. We hypothesized that: 1) Tibetan Plateau might be a hotspot for soil Nr emissions, driven by soil physicochemical properties and microbial nitrogen cycling taxa; 2) atmospheric NO_x and O_3 concentrations inhibit soil Nr emissions due to their effects on soil properties; 3) soil HONO emissions contribute significantly to atmospheric HONO concentrations and further influence atmospheric oxidation capacity in Tibetan Plateau.

2 Materials and Methods

2.1 Soil sampling and property analysis

In this study, 25 soil samples were collected in April 2021 according to different land use types in Linzhi, Tibet (Grassland G1–G4, Cropland C1–C8, Forest F1–F8, Wetland W1– W3, and Bare land BL1–BL2, Fig. S1). The sampling site is located in the southeastern part of the Tibetan Plateau (92°09′E–98°47′E, 26°52′N–30°40′N), where a variety of climatic types coexist, ranging from tropical to frigid. The altitude range was 150–7782 m, with an average elevation of ~3100 m. The annual average temperature, precipitation and sunshine duration are 8.7℃, 650 mm and 2022.2 h, respectively, and the frost-free period was 180 d (Linzhi Municipal People's Government, 2018). At each sampling site, a 10 m × 10 m sample square was delineated, and three sub-samples of topsoil (0–5 cm) were collected along the diagonal, subsequently homogenized to form a composite sample (total weight ~1.5 kg). Subsequently, using a sterile sampling spoon, 1–2 g of soils were collected from the composite sample and placed into 2 mL sterilized centrifuge tubes for subsequent microbiological analysis. The soil samples were transported back to the laboratory within 48 hours via SF Express's standard cold-chain service (maintained at a constant temperature of 4 °C throughout the entire process). Upon arrival at the laboratory, soil samples for microbiological analyses were stored at −80°C, while soil samples for determining Nr gas emissions and physicochemical properties were stored at −20°C.

Soil samples were passed through a 2 mm analytical sieve and used for the determination of physicochemical properties such as soil water content, pH, particle size and inorganic nitrogen. Soil water content (SWC) was calculated by drying at 105°C for 24 h and using the change in soil mass before and after drying. Soil pH was determined by a pH meter (FE28, Mettler Toledo, Zurich, Switzerland) in a soil-water suspension (1:2.5, w/v). Particle size fractions were determined by a laser diffraction particle size analyzer (LA-960A, HORIBA, Kyoto, Japan) (Song et al., 2020). Soil inorganic nitrogen (NO_3^-, NO_2^-, NH_4^+) content was determined by mixing soil with deionized water (DIW) at a ratio of 1:5 (w/v) (Song et al., 2024), shaking and centrifuging, and then the extracted supernatant was analyzed by a continuous flow analyzer (Skalar San++ System, Skalar, Breda, Netherlands) (GB/T 42487-2023). At the same time, another identical sample was incubated in a thermostatic incubator at 25°C for 7 days, and the soil inorganic N content was determined by the method described above, thus calculating the net mineralization rate and net nitrification rate (Lv et al., 2023). For the determination of soil dissolved organic carbon (DOC), 5 g of fresh soil was mixed with 25 mL of 0.5 mol L^{-1} K_2SO_4 solution, shaken for 1 h at room temperature, centrifuged at 4000

r min^{-1} for 5 min through a centrifuge (H1850, Xiangyi, Xiangtan, China). Then the supernatant was extracted by filtration with 0.45 μm aqueous filter membrane, and was analyzed by a total organic carbon analyzer (TOC-L CPN, Shimadzu, Kyoto, Japan). Air-dried soil samples passing a 0.15 mm analytical sieve were measured with an elemental carbon and nitrogen analyzer (Elementary Vario MAX CN, Frankfurt, Germany) to determine the total carbon (TC) and nitrogen (TN) content.

2.2 Soil Nr flux measurement

Dynamic chamber systems were typically used to study the release of Nr (HONO, NO, NO_2, and NH_3) from soils (Behrendt et al., 2014). Here, soil Nr gas fluxes were measured using a MUlti-gaS dynamIC measurement system (MUSIC, Fig. S2). This system simulates soil Nr gas emissions during the wetting-drying cycle and the results are in good agreement with field fluxes and have been applied in several studies (Song et al., 2023; Wu et al., 2020; Wu et al., 2022a; Wu et al., 2019). Specifically, 40 g of fresh soil samples were added to petri dishes (inner diameter = 94 mm) and moistened with purified water until the maximum soil water holding capacity (WHC) was reached, which was measured by filtration (Whatman filter paper no. 42) (Behrendt et al., 2014). Subsequently, the petri dish containing soil was placed in a Teflon chamber (~10 L) in the dark and at a constant temperature (25 ± 0.5°C) and continuously flushed with dry purified air (free of HONO, NO, NO_2, NH_3, O_3, C_xH_y, H_2O, etc.) at a constant flow rate of 6 L min^{-1} until the soil in the petri dish was completely dry. The system was set up with three Teflon chambers, and one of the chambers without soil samples was set up as the reference chamber for calculating the flux. Each chamber was measured for 2 min and then switched to the next chamber via a multipoint switching valve, resulting in a temporal resolution of 6 min per chamber. During the drying process, HONO and NO_2, NO, and NH_3 concentrations in the chamber headspace were measured continuously by incoherent broadband cavity-enhanced absorption spectroscopy (IBBCEAS, AIOFM-CEAS-TY19-1), chemiluminescent NO_x analyzer (Thermo 42i-TL, Waltham, MA, USA), and NH_3 analyzer (Picarro G2103, USA), with instrumental time resolutions of about 10 s, 10 s, and 1 s, respectively. The lower limits of detection (LOD) for instrumental measurements of HONO, NO_2, NO, and NH_3 were approximately 150, 200, 100, and 100 ppt, respectively (Song et al., 2023). In addition to the concentration-based instrument LODs, we have now calculated the minimum detectable fluxes for each target gas. Specifically, the minimum detectable fluxes were approximately 0.8 ng N m^{-2} s^{-1} for NO, 1.6 ng N m^{-2} s^{-1} for NO_2, 0.8 ng N m^{-2} s^{-1} for NH_3, and 1.2 ng N m^{-2} s^{-1} for HONO. To avoid uncertainties caused by switching chambers, only the respective mean value for the 30 s before chamber switching was calculated for each measurement. Furthermore, an infrared CO_2/H_2O analyzer (LI-COR 840A, Lincoln, NE, USA) was used to record soil desiccation and calculate the soil water content (SWC) of the samples.

The fluxes of soil Nr gases (HONO, NO, NO_2, and NH_3) were calculated as follows:

$$F_N = \frac{Q}{A} \times \frac{1}{V_m} \times (x_{out}(t) - x_{in}) \quad (1)$$

where F_N denotes the flux of Nr gases (ng N m^{-2} s^{-1}); Q denotes the flow rate of the gases (m^3 s^{-1}); A denotes the surface area of the soil (m^2); Vm denotes the molar volume of air (m^3 mol^{-1}); t represents the 30 s before chamber switching; and χ_{out} and χ_{in} denote the headspace mixing ratios at the outlet and inlet of the chamber (ppb). The soil sample preservation protocol used

in this study (storage at −20 °C followed by thawing) may have amplified the potential for soil Nr emissions; therefore, we adopted the optimal flux (i.e., the highest value) under specific stimulating conditions, which represents the maximum potential emissions at the maximum WHC.

Meanwhile, based on the above flux data, the integrated soil Nr gases (HONO, NO, NO_2, and NH_3) emission during a single wet and dry alternation were calculated as follows:

$$E_N = \int_{t=0}^{t=\max} F(t) \times \frac{dt}{10^6} \quad (2)$$

where E_N denotes the integrated soil Nr gas emission (mg m^{-2}) and $F(t)$ denotes the soil Nr gas emission flux at moment t. The fluxes were assumed constant over the switch intervals.

2.3 Atmospheric NO_x and O_3 fumigation experiment

Three typical soil types, forest (F3), grassland (G5) and cropland (C2), were selected for the fumigation experiment to simulate the effects of atmospheric NO_x and O_3 concentrations on soil Nr gas emissions. Four fumigation treatments were installed, i.e., 10 ppb NO, 50 ppb NO, 10 ppb NO_x + 30 ppb O_3, and 50 ppb NO_x + 100 ppb O_3. The first two treatments (solely NO) were designed to isolate the direct effect of NO gas on soil nitrogen cycling, independent of its rapid oxidation process, the other two treatments (NO_X + O_3) were designed to simulate the synergistic effects after photochemical aging, where NO is rapidly converted to NO_2 in the presence of O_3, thereby assessing the combined impacts of NO, NO_2, and strong oxidants on the soil system. Although NO rapidly reacts with O_3, and O_3 is concurrently consumed by reactions with soil organic matter, the physicochemical kinetic conditions governing gas conversion and consumption are consistent across all treatment groups under identical flow rates and fumigation regimes. Thus, the relative ranking of actual exposure intensities among the different treatment groups is still considered valid. Three replicates were provided for each treatment, with a total of 36 samples. Specifically, ~100 g of fresh soil samples were weighed and placed into 500 mL brown incubation flasks (Bottom diameter: 7.5 cm; Bottle height: 17.5 cm; Soil thickness: 3–5 cm). The NO standard gas (5.2 ppm, Air Liquide, Shanghai) was subsequently diluted to a pre-set NO/NO_x+O_3 mixing ratio concentration by the Sonimix ozone gas master standard (SONIMIX 4001, LNI, Italy) and piped into an incubation bottle containing soil (flow rate ~3 L min^{-1}) (Fig. S3). The lid of the incubation bottle was equipped with two connecting pipes and loaded with valves that enable controlled on/off switching. The second pipe of the incubation bottle was connected to the NO_x analyzer to allow real-time observation of changes in NO_x concentration in the bottle. When the fumigant gas in the bottle reaches the pre-set concentration, promptly close the valve of the pipeline connected to the instrument. The whole process will take about 5 min. Then, the soil was fumigated for another 10–20 s before closing the valve of the fumigant gas input pipe. The tube junction was sealed with a sealing film and then placed in a thermostatic incubator (25 ± 0.5°C). Based on the results from preliminary tests, we selected a fumigation period of 5 days (Table S1), during which the fumigant gas input was repeated every 24 h to ensure a stable concentration of fumigant gas in the incubation bottles. After fumigation incubation was completed, ~2 g of soil samples were collected within 3 min into 2 mL sterilized centrifuge tubes, and then placed in a refrigerator at −80°C for storage for subsequent soil microbial analyses. In

addition, ~40 g of soil samples were removed from the incubation bottles for the determination of Nr flux. The remaining samples were used for the determination of soil pH, inorganic nitrogen content, and DOC content.

2.4 Soil DNA extraction and sequencing

DNA was extracted from 25 natural soil samples using a DNA extraction kit (MOBIO Laboratories, Carlsbad, CA, USA). The concentration and quality of DNA were determined by NanoDrop2000 (Thermo Fisher Scientific, Waltham, Massachusetts USA) and 1% agarose gel electrophoresis. The primer pairs 338F (5'-ACTCCTACGGGAGGCAGCAG-3') and 806R (5'-GGACTACHVGGGTWTCTAAT-3'), 524F10extF (5'-TGYCAGCCGCCGCGGTAA-3') and Arch958RmodR (5'-YCCGGCGTTGAVTCCAATT-3'), ITS1F (5'-CTTGGTCATTTAGAGGAAGTAA-3') and ITS2R (5'-GCTGCGTTCTTCATCGATGC-3') for bacterial V3-V4 region, archaeal V4-V5 region, and fungal ITS1-ITS2 region by PCR amplification (GeneAmp®9700 PCR Thermal Cycler, ABI, CA, USA), respectively. The volume of the PCR reaction system was 20 μL, see Table S2 for specific reagents and volumes. The PCR amplification cycling conditions were: pre-denaturation at 95°C for 3 min, followed by denaturation at 95°C for 30 s, annealing at 55°C for 30 s, extension at 72°C for 45 s for a total of 35 cycles, and finally extension at 72°C for 10 min until 10°C. In 3 replicates per sample, PCR products from the same sample were mixed and detected by 2% agarose gel electrophoresis and purified using the AxyPrep DNA Gel Extraction Kit (Axygen Biosciences, Union City, CA, USA) according to the manufacturer's instructions, and Quantus™ fluorometer (Promega, USA) was used to quantify. Library construction of purified PCR products was performed using the NEXTFLEX® Rapid DNA-Seq Kit. Finally, the library was subjected to paired-end sequencing on the Illumina MiSeq PE300 platform (Meiji Biomedical Technology Co., Ltd., Shanghai, China). Raw sequencing data were uploaded to the Scientific Data Centre of Beijing Institute of Genomics, Chinese Academy of Sciences (https://ngdc.cncb.ac.cn/gsub/submit/gsa/subCRA019428/finishedOverview) under the accession number CRA012324.
The raw sequencing sequence of the double-end was quality controlled using Fastp software (V0.19.6, https://github.com/OpenGene/fastp) and spliced using FLASH software (V1.2.11, https://ccb.jhu.edu/software/FLASH/index.shtml). Using UPARSE software (V11, http://www.drive5.com/uparse/), the quality-controlled spliced sequences were clustered by operational taxonomic unit (OTU) and chimeras were excluded based on 97% similarity. The RDP classifier (V2.13, https://sourceforge.net/projects/rdp-classifier/) was used to compare the Silva 16S rRNA gene database (V138, https://www.arb-silva.de/) as well as the Unite fungal ITS database (V8, https://unite.ut.ee/) for OTU species taxonomic annotation with a confidence threshold of 70%, and the community composition of each sample was counted at different species classification levels.

2.5 Quantification of functional genes involved in nitrogen cycling

Natural soil DNA was extracted from 0.25 g of frozen soil using the MoBio PowerSoil DNA Kit (MOBIO Laboratories) and fumigated soil DNA was extracted from 0.25 g of frozen soil using the DNeasy® PowerSoil® Pro Kit (QIAGEN, USA). Quantitative real-time PCR (qPCR) (7300 Real-Time PCR System, Applied Biosystems, USA) was performed on natural soil

DNA samples using SYBR fluorescent dye quantitative PCR to determine the copies of *amoA*, *narG*, *nirK*, *nosZ* and *napA* genes. The qPCR reaction mixture for natural soil consisted of 2 μL Template DNA, 0.8 μL forward and reverse primers, 10 μL 2×ChamQ SYBR Color qPCR Master Mix (Vazyme), 0.4 μL 50×ROX Reference Dye 1 and 6 μL ddH_2O. Fumigated soil DNA samples were also used by SYBR fluorescent dye method for qPCR (7500 Real-Time PCR System, Applied Biosystems, USA) to determine the copies of *amoA*_AOA, *amoA*_AOB, comammox Clade A, *nirK*, *nirS*, *nxrA*, *nxrB*, *napA*, and *nosZ* genes. The qPCR reaction mixture for fumigated soil consisted of 1 μL Template DNA, 0.4 μL forward and reverse primers (0.8 μL for comammox Clade A and *napA* genes), 10 μL 2×TB Green Premix Ex Taq (Takara), 0.4 μL 50×ROX Reference Dye II and 7.8 μL ddH_2O (7 μL for comammox Clade A and *napA* genes). Primer sets and qPCR conditions for each gene were listed in Table S3. A qPCR standard curve based on threshold cycling (CT) values was constructed using a 10-fold dilution of the linearized plasmid. The gene copies of each soil sample were then determined by correlating the CT value of each sample with the known copies in the standard curve using a known linear logarithmic relationship. Plasmid copies conversion formula (copies μL^{-1}) = plasmid concentration (ng μL^{-1}) × 10^{-9} × 6.02 × 10^{23} / (molecular mass × 660). The amplification efficiencies of all qPCRs in this study were in the range of 80%–110% and $R^2 > 0.99$ (Table S3).

2.6 Upscaling soil emissions of Nr gases to the Tibetan Plateau

We compiled a dataset of soil Nr fluxes in Tibet, including measured data in this study and published data in literature (Table S4). Stepwise regression analysis was performed to establish quantitative relationships between soil Nr fluxes and key soil properties, including soil pH, inorganic nitrogen contents, and the abundance of nitrogen-cycling functional genes. Based on these relationships and the flux dataset, we estimated the annual soil emissions of HONO, NO, and NO_x in Tibet using parameterized soil Nr emissions model (Wu et al., 2022b). This model takes into account factors such as soil temperature, precipitation, and nitrogen fertilizer application (on farmland). It should be clarified that the current annual emission model does not directly incorporate the effects observed in the fumigation experiments. The upscaling model relies on statistical relationships established between soil Nr fluxes and key in-situ soil properties. While these long-term in-situ properties inherently reflect historical deposition, capturing the short-term chemical feedback of ambient NO_x/O_3 into a regional-scale model is complex. Thus, these effects are qualitatively discussed in relation to the fumigation results (Figs. S5–S7).

2.7 Quantification the contribution of soil HONO emissions to atmospheric external HONO sources

We quantified the contribution of soil HONO emissions to NO_x-independent (external) atmospheric HONO sources by integrating the external source framework of Wang et al. (2023a) with the soil-atmosphere exchange model of Meusel et al. (2018), based on field data collected at the Nam Co Multisphere Observation and Research Station (30°46.44′N, 90°59.31′E, 4730 m a.s.l.) (Wang et al., 2023a). Here, community-weighted maximum HONO flux ($F_{comm,max}$) was calculated by weighting land-use-specific maximum HONO fluxes by their areal coverage (bare soil: 12%; grassland: 74%; cropland: 0.1%; forest: 9%; wetland: 5.6%) (Yang and Huang, 2025):

$$F_{comm,max} = \sum_{i=1}^{n} F_{max,i} \times \frac{p_i}{100} \quad (3)$$

where $F_{max,i}$ = maximum HONO flux for land-use type i (ng N m^{-2} s^{-1}); p_i = areal percentage of land-use type i. Land-use-specific $F_{max,i}$ values were: bare soil (21.6 ± 8.4); grassland (18.3 ± 6.2); cropland (42.1 ± 28.1); forest (15.7 ± 5.3); wetland (9.8 ± 3.7) ng N m^{-2} s^{-1}.

Soil HONO molecular flux normalized to boundary layer volume ($S_{ground,cm^{-3}}$) was calculated as:

$$S_{ground,cm^{-3}} = \frac{F_{comm,max} \times a}{BLH \times 10^6} \quad (4)$$

where a = unit conversion factor; 10^6 = scaling to cm^3; BLH (boundary layer height) of 182 m was used derived from ERA5 reanalysis data for Nam Co station. A constant BLH is a simplification. The 182 m daily-average from ERA5 for Nam Co was adopted to focus on daytime oxidation capacity driven by HONO photolysis.

The volume mixing ratio production rate S_{mix}(pptv h^{-1}) representing soil HONO contributions to atmospheric external sources was derived as:

$$S_{mix} = S_{ground,cm^{-3}} \times k \quad (5)$$

where k = 3.11×10^{-4} pptv h^{-1}per molecules $cm^{-3}s^{-1}$, calculated using the ideal gas law, calibrated based on the air molecular number density (1.159×10^{19} cm^{-3}) and Nam Co's in-situ meteorology (mean daytime temperature: 278.15 K; average atmospheric pressure: 4.45×10^4 Pa) to account for high-altitude thermodynamic properties.

2.8 Statistical analysis

Kruskal-Wallis test, and one-way analysis of variance (ANOVA) and Duncan's multiple comparisons (SPSS Version 26.0., IBM Corp., Armonk, NY, USA) were used to distinguish the differences of soil physicochemical properties, functional genes, microbial community diversity and Nr fluxes for different soil use types and fumigated soils, respectively. Non-metric multidimensional scaling (NMDS), analysis of similarity (ANOSIM) and non-parametric multivariate analysis of variance using distance matrices (ADONIS) were used to reveal differences in the composition of archaeal, bacterial and fungal communities across soil use types (R V3.6.3, "vegan" package, https://www.r-project.org/). Spearman correlation analysis resolved the relationship between physicochemical properties, functional genes, microbial communities and Nr fluxes in Tibetan soils, while Pearson correlation analysis was applied to resolve the relationships in fumigated soils. Both methods were performed using Origin 2023.

3 Results and Discussion

3.1 Soil physicochemical properties, microbial communities and functional genes abundance

Tibetan region has remarkable differences in physicochemical properties among different soil types, such as pH, TN, TC, C/N ratio, NH_4^+-N, particle size, and moisture ($p < 0.05$, Table S5). In this study, we detected that pH was alkaline in bare soil (8.14 ± 0.18) and wetland (7.84 ± 0.19), acidic in grassland (5.10 ± 0.19) and cropland (6.36 ± 0.64), whereas in forest pH

(4.76–8.16) had a wide range of distributions in the Tibetan region, generally in accordance with the results of other studies (Ma et al., 2020; Wang et al., 2023b; Yang et al., 2021). Soil clay content was low (≤1%), with essentially consisting of silt and sand in all soils (Table S5). It has been reported that carbon and nitrogen storage is substantial in surface soils of the Tibetan Plateau, particularly in grasslands (Chen et al., 2022a). Similar results were also obtained in this study, with the TN and TC contents of grassland being 3–26 times more than other soil types (Table S5). Agricultural soils showed comparatively higher NO_3^--N content and N transformation rate (net mineralization and nitrification rate) than other soil types, indicating fast N turnover effects caused by fertilization. In addition, Tibetan soils had elevated NO_3^--N content compared with NO_2^--N and NH_4^+-N content, which was similar to the results of other studies (Gao et al., 2016; Lin et al., 2019; Yao et al., 2019). Overall, 1202964, 1079854 and 1589093 high-quality bacterial, archaeal and fungal gene sequences were detected from 25 soil samples, respectively. The sequences were clustered with 97% similarity to obtain 8355, 531 and 5806 OTUs (Table S6). The Shannon-Wiener dilution curve was flattened, indicating that the sequencing volume was able to reflect most of the microbial diversity information in the soil samples (Fig. S4) (Wang et al., 2012; Wu et al., 2022a). The number of shared species of bacteria, archaea, and fungi across all soil types was 878, 46, and 75, respectively. However, archaea (average ~71) and fungi (average ~778) had more unique species than shared species in different soil types (Table S7). In general, microbial community alpha-diversity was assessed in terms of richness, evenness, diversity and coverage, while community beta-diversity reflected differences in species composition between populations via comparisons of species composition structure between samples (He et al., 2013). In this study, the Good's coverage indices of bacterial, archaeal and fungal communities all ranged from 0.97 to 0.99 (Table S8), indicating that the results of the current sequencing were highly plausible. It was found that the diversity and community structure of soil archaea, bacteria and fungi were moderately heterogeneous among the different soil types (Kang et al., 2021). This study revealed that archaeal community richness and fungal community richness, evenness and diversity were statistically different between soil types, whereas bacterial richness, evenness and diversity did not differ significantly (Fig. 1a). Meanwhile, based on the results of NMDS ordination (Fig. 1b) and statistical analyses (Table S9, $p<0.05$), it was shown that beta-diversity of bacteria, archaea, and fungi varied significantly across soil types, in particular between cropland soils and other soil types. The results demonstrated that soil habitat specificity shaped the diversity of soil microbial communities on the Tibetan Plateau.

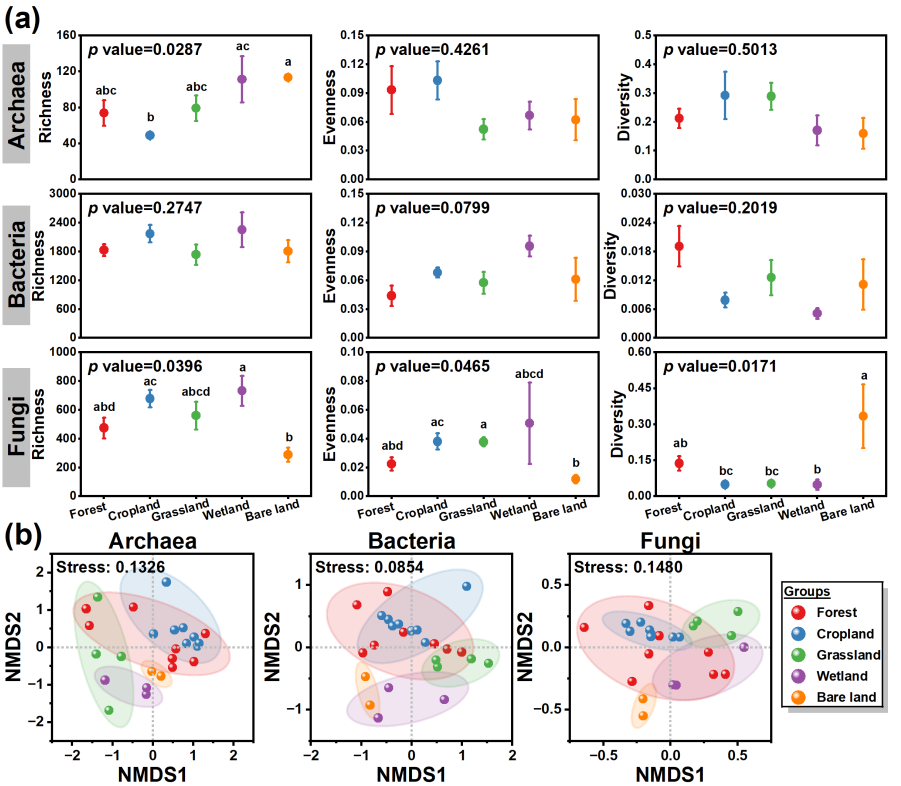

Figure 1: Soil archaeal, bacterial and fungal communities of α-diversity (a) and β-diversity (b). The error bars show the standard errors (Forest: *N*=8; Grassland: *N*=4; Cropland: *N*=8; Wetland: *N*=3; Bare land: *N*=2). Kruskal Wallis test was used for one-way ANOVA between groups, and different lowercase letters show differences between groups. Richness is actual observations; evenness is based on Simpson's index measure; diversity is Simpson's diversity index.

Through the sequencing results, soil bacteria, archaea and fungi were affiliated to 50, 12 and 17 phyla, respectively (Table S6). Fig. 2a showed that the soil archaeal community was dominated by Crenarchaeota (10%–99%), Thermoplasmatota (0%–59%), Euryarchaeota (0% –62%), and Halobacterota (0%–47%) in the soil archaeal community. The dominant phyla of the bacterial community were Actinobacteriota (6%–65%), Proteobacteria (13%–46%), Acidobacteriota (3%–25%), Chloroflexi (3%–21%), and Firmicutes (1%–23%). The dominant phyla of the fungal community were Ascomycota (1%–90%), Basidiomycota (0%–69%), Mortierellomycota (0%–84%), and Chytridiomycota (0%–62%). It was similar with other studies reporting the composition of soil microbial communities on the Tibetan Plateau (Cao et al., 2022; Cao et al., 2021; Yang et al., 2022; Zou

et al., 2023). Crenarchaeota predominated in the Tibetan soil archaeal community, especially in cropland soils (average relative abundance ~98%), far above other soil types. Additional studies confirmed that Crenarchaeota extensively exist in marine, hot spring and soil environments, which constitute the most numerous and widespread ammonia-oxidising archaeal taxa in nature, with the ability to oxidize ammonia to nitrite for chemoenergetic autotrophic growth, thus being critical for nitrogen fertiliser utilization (Baker et al., 2020; Brochier-Armanet et al., 2008; Dang et al., 2008). Further clarification was provided to explain the low NH_4^+-N content and high net mineralization/nitrification rates in croplands in Tibet (Table S5). It was found that Actinobacteriota genomes harboured numerous functional genes related to plant residue degradation, and that Ascomycota fungi exhibited the ability to degrade multiple types of plant cellulose and hemicellulose, which increased nitrogen availability during microbial-driven decomposition of plant residues (Bao et al., 2021; Swarnalakshmi et al., 2016; Zhang et al., 2013). Thus, those in cropland soils with high abundance of Actinobacteriota (average relative abundance ~ 36%) and Ascomycota (average relative abundance ~ 54%) presumably provide additional nitrogen for themselves and other microorganisms. Meanwhile, the abundance of key functional genes for N cycling in grassland and cropland soils was higher than that in other soil types, with *napA*, *narG*, *nirK*, and *nosZ* gene abundance higher in grassland soils, and *amoA* gene abundance higher in cropland soils, whereas all of the above genes had lower abundance in bare soils (Fig. 2b). This indicated that grassland and cropland soils in the Tibetan Plateau region possessed high nitrification and denitrification potentials.

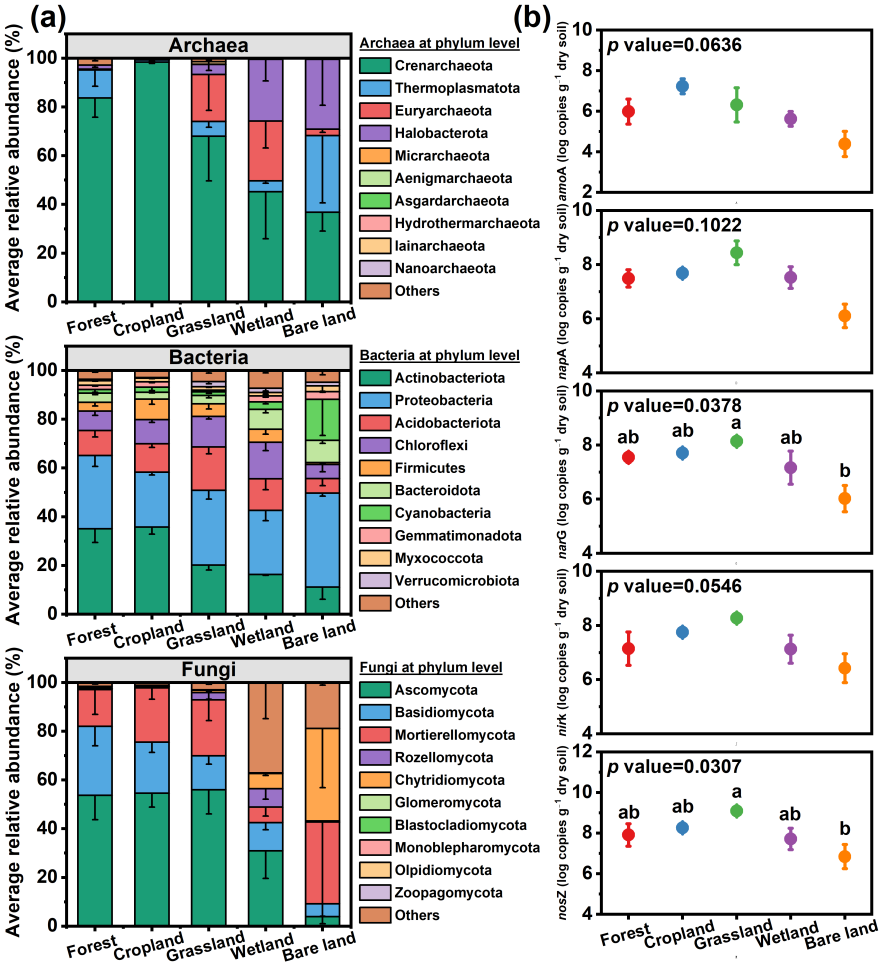

Figure 2: Soil Archaea, Bacteria, and Fungi Community Composition (a) and Functional Genes (b). The error bars show the standard errors (Forest: N=8; Grassland: N=4; Cropland: N=8; Wetland: N=3; Bare land: N=2). The figure shows the top 10 phyla in relative abundance of soil archaea, bacteria and fungi. Kruskal Wallis test was used for one-way ANOVA between groups, and different lowercase letters show differences between groups.

3.2 Soil Nr emissions characteristic and driving factors

Under natural conditions, soil–atmosphere exchange of reactive nitrogen is typically bidirectional (Bao et al., 2022). Here, we quantify net soil emissions and eliminate the masking effect of atmospheric Nr background by using dry Nr-free air as the carrier gas. For example, the observed HONO flux represents the net apparent flux, which integrates direct soil biogenic emission and additional HONO formation via heterogeneous uptake and conversion of atmospheric NO_2 on soil particle surfaces (Fan et al., 2025). This dual-source characteristic helps explain the co-occurrence of HONO release and NO_2 consumption observed in Fig. 3. It is important to acknowledge the methodological limitations regarding the interpretation of our flux results. In this study, all soils were found to emit of HONO, NO, NO_2 and NH_3 during wetting and drying cycles (Fig. 3). The optimum fluxes ranged from 2.5 to 235.2 ng N m^{-2} s^{-1} for HONO, 1.2 to 268.4 ng N m^{-2} s^{-1} for NO, 7.6 to 43.7 ng N m^{-2} s^{-1} for NO_2, and 6.4 to 547.8 ng N m^{-2} s^{-1} for NH_3 (Fig. 3a). Integrating the single wetting and drying cycle, the release of HONO was 0.02–0.30 mg N m^{-2}, NO was 0.01–0.51 mg N m^{-2}, NH_3 was 0.47–3.07 mg N m^{-2}, and NO_2 was < 0 (Fig. 3b). When compared to studies with similar conditions or methods, the emissions in this study were consistent with those reporting soil HONO, NO, or NO_2 emissions ranging from 1 to 3000 ng N m^{-2} s^{-1} (Mamtimin et al., 2016; Meusel et al., 2018; Oswald et al., 2013; Song et al., 2023; Su et al., 2011; Weber et al., 2015; Wu et al., 2022a; Wu et al., 2019). Optimal fluxes and integrated emissions of HONO, NO and NO_2 showed high consistency and convergence across cropland soils. Cropland soils consistently remained the primary source of HONO, NO and NO_2 emissions (42.1 ± 28.1, 49.2 ± 31.8 and 19.9 ± 3.6 ng N m^{-2} s^{-1}, respectively), whether in terms of instantaneous peaks or cumulative emissions. The findings suggest that the emission mechanisms in cropland ecosystems for HONO, NO, and NO_2 are relatively continuous over time and highly stable (Fig. 3). Studies have shown that high Nr gas emissions from cropland soils depend strongly on fertiliser application factors (Luo et al., 2022). Nitrogen fertiliser application promoted strong HONO emissions, the flux of HONO from fertilised agricultural soils can exceed 1000 ng N m^{-2} s^{-1} (Tang et al., 2019; Xue et al., 2021; Xue et al., 2019). In addition, it has been shown that fertilization or grazing increased soil HONO emissions, which were expressed as farmland ≥ grassland ≥ forest and peatland for different soil types (Bhattarai et al., 2021). It is worth noting that the substantial NO_2 emissions observed in this study cannot be fully explained by classical microbial nitrification and denitrification mechanisms alone. Apart from biological pathways, direct NO_2 emissions are likely driven by several abiotic or non-classical biotic mechanisms. Chemodenitrification is recognized as a significant source of NO_2 in soils; specifically, under acidic conditions, the accumulated NO_2^- in soil undergoes chemical decomposition to produce NO and NO_2 (Cai et al., 2012).

However, it should be noted that extrapolating the results of this study to actual field conditions has inherent limitations. Xue et al. (2024) showed that surface water exchange plays a critical role in mediating soil Nr emissions. Under the dry-air conditions employed in our experimental setup, the evaporation of surface water is likely maximized. This enhanced evaporation could potentially facilitate the escape of dissolved Nr gases from the soil matrix, thereby leading to an overestimation of the net fluxes compared to ambient conditions with higher relative humidity. Therefore, our findings provide theoretical maximum emission potentials, and caution is advised when directly applying the absolute flux magnitudes obtained

here to field assessments without considering local in situ environmental data (e.g., soil moisture, temperature). Future studies integrating in situ field measurements or environmentally controlled microcosm systems are essential to delineate the dynamic impacts of wet-dry cycles on Nr emissions.

Spearman's correlation analysis revealed that the potential of soil Nr gas emission in Tibet was remarkably correlated with soil physicochemical properties, microbial communities and key functional genes of the nitrogen cycle (Fig. 4, $p<0.05$). Generally, soil HONO and NO emissions were significantly correlated with soil pH and nitrogen content. Su et al. (2011) found that HONO emissions increased with higher nitrogen content and acidity in the soil. In contrast, Oswald et al. (2013) measured soil HONO emissions under different pH conditions globally and found that the fluxes did not decrease with increasing pH. Furthermore, another study demonstrated that the pH at the surface of soil mineral particles, rather than the pH of the soil solution, influences soil HONO emissions (Donaldson et al., 2014). Meusel et al. (2018) reported that HONO and NO emissions were significantly correlated with soil NO_3^- and NO_2^-. Wu et al. (2022b) found that HONO and NO emissions from different types of soils in Shanghai had been correlated remarkably with the concentrations of NH_4^+, NO_3^- and NO_2^- concentrations. Nevertheless, in this study, soil HONO was significantly correlated with *amoA* gene abundance and archaeal evenness, while soil NO was significantly correlated with *amoA*, *narG*, *nirK*, and Actinobacteriota abundance (Fig. 4, $p<0.05$). Wu et al. (2022a) found that *amoA*_AOA abundance directly affected the wetland soil HONO emission, while NO emission were mainly controlled by *amoA*_AOA, *nirK* and *nirS* genes. In this instance, soil nitrification rate was dictated by AOA and negatively correlated with the C/N ratio, particularly when the C/N ratio exceeds 25 (Maljanen et al., 2013; Mushinski et al., 2019). At this threshold, soil HONO and NO emissions decreased rapidly. Additionally, the fluxes of HONO and NO were affected by AOB, which influenced *amo* gene abundance through soil pH, subsequently impacting soil HONO emissions (Mushinski et al., 2019; Scharko et al., 2015).

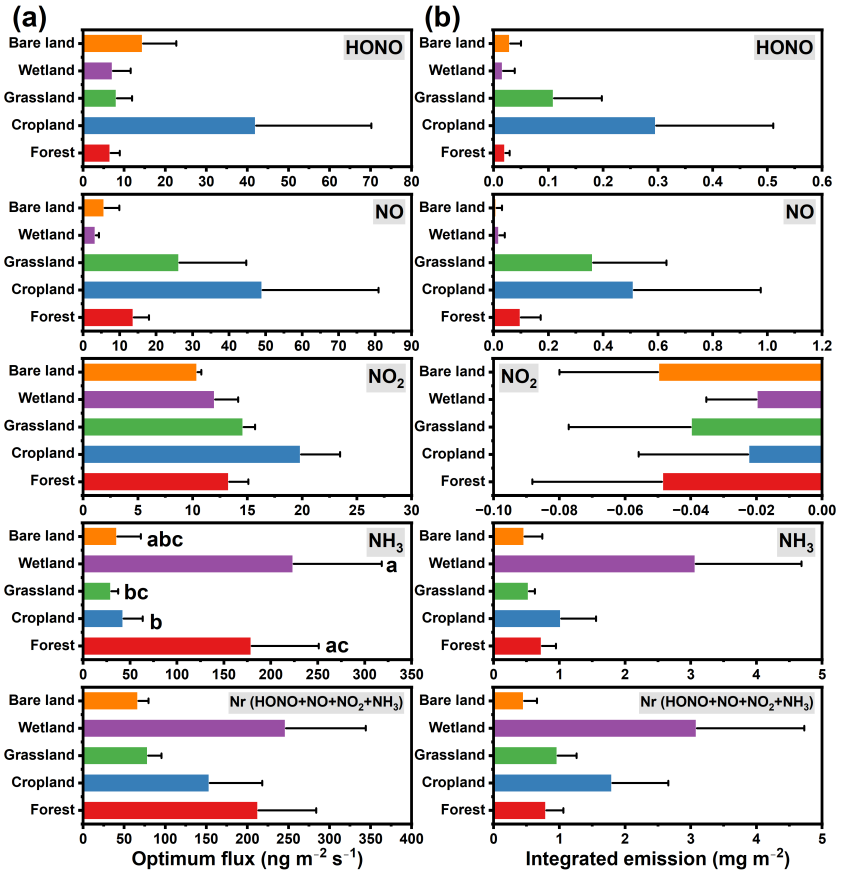

Figure 3: Optimum flux (a) and integrated emissions (b) of soil Nr gases (HONO, NO, NO_2, NH_3). The error bars show the standard errors (Forest: N=8; Grassland: N=4; Cropland: N=8; Wetland: N=3; Bare land: N=2). Kruskal Wallis test was used for one-way ANOVA between groups, and different lowercase letters show differences between groups.

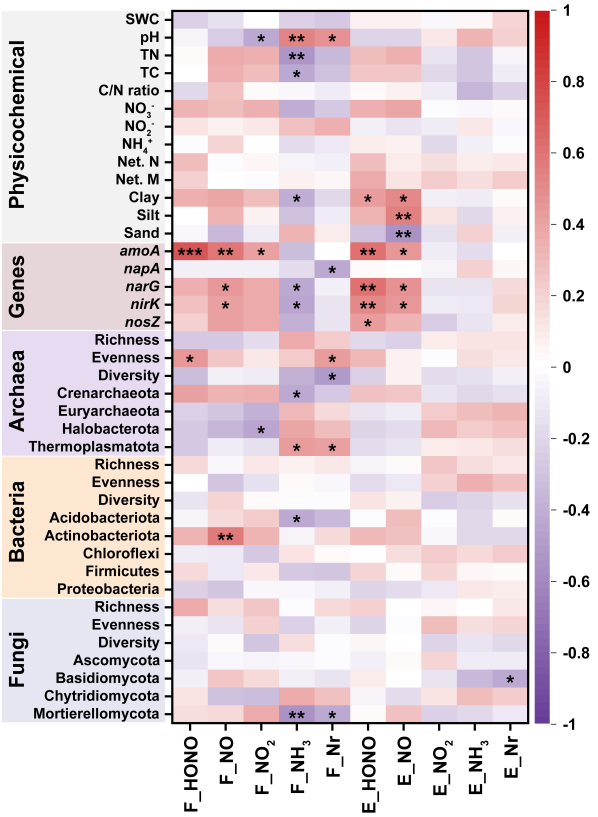

Figure 4: Correlation matrix between soil physicochemical properties, functional genes, microbial communities and Nr fluxes based on Spearman correlation analysis. SWC: Soil water content; TN: total nitrogen; TC: total carbon; C/N ratio: TC/TN; Net. N: net nitrification rate; Net. M: net mineralization rate; Richness is actual observations; evenness is based on Simpson's index measure; diversity is Simpson's diversity index. * $P < 0.05$; ** $P < 0.01$; *** $P < 0.001$.

Actinobacteria belong to Gram-positive bacteria, which can degrade soil organic matter, provide nutrients to the soil, as well as maintain high activity and DNA repair ability even at low temperatures, acting as a dominant group of bacteria in low-temperature environments (Johnson et al., 2007). In our study, we also found Actinobacteriota (6%–65%) to be the dominant phylum of the bacterial community in Tibet, especially in cropland soils (Fig. 2a). High NO emissions from cropland soils showed a strong consistency with Actinobacteriota abundances. Therefore, it is suggested that Actinobacteriota may act as a

significant microbial regulator for NO emissions in Tibetan cropland soils. Overall, soil reactive N emission potential in Tibet was explained by soil pH, carbon and nitrogen content, (de)nitrification functional genes, and key microflora.

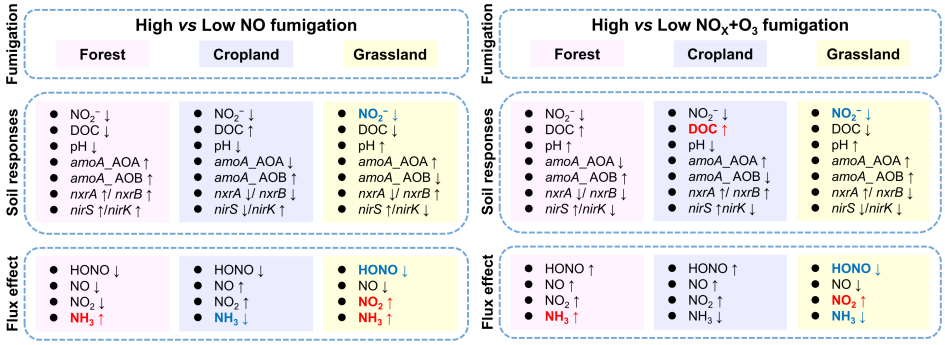

Figure 5: Conceptual diagram linking the effects of fumigation with high and low concentrations of NO and NO_X+O_3 on soil microbial functional genes, physicochemical properties, and Nr fluxes across forest, grassland, and cropland soils. Red bold indicate statistically significant increases, while blue bold indicate statistically significant decreases.

Atmospheric Nr emissions and deposition rates have been highly elevated in China during recent years, and studies have shown that a shift towards approximately equal wet and dry nitrogen deposition occurred in 2011–2015, accompanied by increasing dry nitrogen deposition (Liu et al., 2020; Yu et al., 2019; Zhu et al., 2022). Total N emissions from terrestrial ecosystems to be 100 Tg N yr^{-1}, with an eventual 70 Tg N yr^{-1} being deposited back into terrestrial ecosystems (Fowler et al., 2013). Total annual input of atmospheric nitrogen dry deposition in China was 7.78 kg N ha^{-1}, of which the annual deposition flux of NO_2 was 0.67 kg N ha^{-1} (Jia et al., 2016). In this study, we found that exposure to simulated atmospheric NO_x/O_3 concentrations altered soil Nr emissions, while HONO and NO emissions from different soil types responded differently to NO_x/O_3 fumigation with different concentration gradients (Figs.5 and S5–S7). Specifically, the HONO and NO emissions from forest soils were enhanced after NO and NO_x/O_3 mixture fumigation, which resulted in peak emissions that were 2–8 times higher than the previous levels (Fig. S5). However, HONO and NO emissions from cropland and grassland soils were suppressed by fumigation, with HONO and NO peaks in cropland soils decreasing by an average of approximately 31% and 31% (Fig. S7), while HONO and NO peaks in grassland soils were decreased by an average of approximately 68% and 84% (Fig. S6). Interestingly, while cropland and grassland soils typically serve as sources of HONO and NO under natural conditions, their fluxes were significantly suppressed under fumigation with elevated NO and NO_X + O_3. These results indicate that high concentrations of NO and NO_X + O_3 may lead to a decrease in the soil production rates of HONO and NO, thereby causing a reversal of the source-sink balance. Previous study showed that the net atmospheric Nr budgets for paddy fields, forests, and tea plantations in a sub-tropical catchment to be +3.7, −36.1, and +23.8 kg N ha^{-1} yr^{-1}, respectively, suggesting that forests served as sinks of atmospheric Nr, whereas paddy fields and tea plantations served as sources of atmospheric Nr (Zhu et al.,

2021). In addition, forests have a higher efficiency of atmospheric nitrogen capture than other land-use types (Du et al., 2019). Therefore, forest soils under NO_x/O_3 exposure might absorb more inputs from external nitrogen sources, accelerating the rate of nitrogen transformation under the dry-wet cycle, which led to increased emissions of HONO and NO.

Fumigation with different concentration gradients of NO and NO_x/O_3 also altered soil physicochemical and biological properties (Fu et al., 2020; Ning et al., 2015). Forest (pH ~5.59 ± 0.16), cropland (pH ~5.44 ± 0.18) and grassland (pH ~5.10 ± 0.05) soils were acidic before fumigation in the study. It was found that soil pH tended to increase after fumigation, especially in forest soils, with an average increase of ~0.53 (Fig. S8). The increase in pH is primarily attributed to changes in the redox state, H^+ consumption during the reduction of nitrogen intermediates, and shifts in microbial functional communities (Chen et al., 2023; Slessarev et al., 2016; Wu et al., 2026). Under strong oxidative fumigation conditions, the abundance of denitrification genes increased (Fig. S8), which likely led to greater H^+ consumption, thereby raising the soil pH. Furthermore, the differential responses among soil types, rather than a uniform shift across all treatments, suggest that the pH increase was predominantly driven by the fumigation gases rather than merely by the duration of laboratory incubation. Fig. S9 results showed that soil pH was remarkably positively correlated with HONO and NO emissions ($p < 0.001$), in agreement with the findings of (Scharko et al., 2015). Therefore, soil pH increased probably one reason for the increased emissions of HONO and NO from forested soils under fumigation. Moreover, it has also been shown that soils with pH near neutrality were capable of more HONO emissions (Oswald et al., 2013). While atmospheric nitrogen deposition, as a new nitrogen input to terrestrial ecosystems, possibly causes an increased soil carbon storage (Bala et al., 2013; Magnani et al., 2007), consistent with the results of this study on increased soil DOC content under fumigation. It was shown that atmospheric nitrogen deposition decreased the soil C/N ratio, facilitated the mineralization of organic matter in the soil, increased the accumulation of inorganic nitrogen in the soil (Fu et al., 2020; Lu et al., 2011). This phenomenon was seen in cropland soils, where increased NO_3^- and NH_4^+ content was found at elevated fumigation concentrations (Fig. S8). The results showed that under NO and NO_x/O_3 fumigation, cropland soils possibly preferred to undergo mineralization and nitrification processes, which resulted in higher nitrogen accumulation and lower gaseous losses, consistent with the results of the Nr emissions we measured (Fig. S7). Grassland soils under high concentration of NO fumigation increased pH and decreased NO_2^- content, which was not beneficial to soil HONO emissions in this condition, as well as raised NO_3^- content indicating that grassland soil tended to undergo the process of NO_3^- accumulation more than NO_3^- consumption under high concentration of fumigation (Figs. 5 and S8). Therefore, HONO and NO emissions from grassland soils under NO and NO_x/O_3 fumigation tended to decrease (Figs. 5 and S6). Functional microbial genes associated with nitrogen cycling in forest soils were sensitive to nitrogen addition (Levy-Booth et al., 2014). In this study, the abundance of *nxrB*, *nirK* and *nirS* genes was altered in forest soils under different concentration gradients of NO and NO_x/O_3, which increased significantly under high NO_x/O_3 fumigation, resulting in the decomposition of more NO_3^- and NO_2^-, thereby releasing more HONO and NO (Figs. S5 and S8). It should be noted that the effects observed in the fumigation experiments (Figs. S5–S7) are discussed qualitatively but are not incorporated into the annual emission parameterization. The annual model relies on long-term in-situ soil properties, which makes it challenging to extrapolate short-term chemical feedback to a regional scale. Therefore, this qualitative discussion highlights the complex interplay between

atmospheric chemistry and soil biogeochemistry. Furthermore, exposure to elevated NO_x/O_3 also affected the diversity and composition of soil microorganisms, as well as the key flora involved in the nitrogen cycle, all of which were also related to soil Nr gas emissions (Berthrong et al., 2014; Fierer et al., 2012; Leff et al., 2015; Treseder, 2008; Wang et al., 2018; Zhang et al., 2018b). However, this study has not obtained the relevant data, which leads to the limitation of the study modeling the effects of atmospheric NO_x/O_3 exposure on soil Nr gas emission.

3.3 Regional soil HONO and NO emissions and atmospheric implications

The annual emissions of soil Nr gases in Tibet were estimated as 7.0 ± 3.4 Gg N yr^{-1} for HONO, 11.6 ± 7.8 Gg N yr^{-1} for NO, and 20.3 ± 7.0 Gg N yr^{-1} for NO_x in 2021, respectively (Fig. 6 and Table S10). These emissions were lower with the recently reported HONO value of 12.3 Gg N yr^{-1} but higher than the NO_x value of 8.9 Gg N yr^{-1} for 2015 (Li et al., 2026). This discrepancy arises mainly from improved model inputs in this study, including in-situ soil moisture and microbial activity data, in contrast to statistical interpolation with sparse field observations in previous work.

By land-use type, bare soils are the largest contributor due to their vast coverage (43% of land area), accounting for 43% of HONO (3.0 ± 2.0 Gg N yr^{-1}), 46% of NO (5.3 ± 4.2 Gg N yr^{-1}), and 67% of NO_x (13.6 ± 3.6 Gg N yr^{-1}) emissions. This aligns with studies highlighting high Nr emissions from desert soils and biological soil crusts (Bhattarai et al., 2021; Meusel et al., 2018). Grasslands contribute 29% to HONO and 44% to NO emissions. Our estimated grassland NO emission of 0.2 (0–1.7) kg N ha^{-1} yr^{-1} is comparable with previous plateau studies (Gao et al., 2016; Holst et al., 2007; Lin et al., 2019; Yao et al., 2019; Zhang et al., 2018a). Croplands, despite having the highest fluxes per unit area (Fig. 3), contribute only 8% to HONO emissions (0.5 ± 0.1 Gg N yr^{-1}) due to their limited spatial extent (~0.3%). This contrasts with global patterns where croplands are often the dominant source (Wu et al., 2022b), highlighting the unique emission profile of the Tibetan Plateau where natural ecosystems prevail. To validate our estimates, the upscaling model integrated both measured and published field data from the Tibetan Plateau (Table S4). Our HONO and NO_x estimates are consistent with recent regional bottom-up inventories (Li et al., 2026; Wu et al., 2022b) and provide useful constraints for GEOS-Chem simulations over the Third Pole (Wang et al., 2025a).

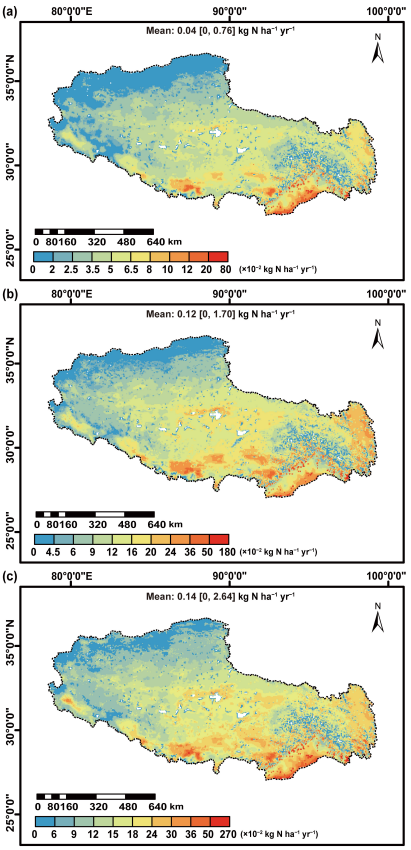

Figure 6: Spatial distribution of annual emissions of HONO (a), NO (b), and NO_x (c) from soils in Tibet. The values in bracket show the minimum and maximum emissions.

To quantify the contribution of soil HONO emissions to the atmospheric budget, we integrated our flux data with observations from the Nam Co Multisphere Observation and Research Station. Our optimized calculation framework, combining the external source definition and the soil-atmosphere exchange model (Meusel et al., 2018), reveals that soil HONO emissions on the Tibetan Plateau produce a volume mixing ratio of 10.5 pptv h^{-1}. This accounts for approximately 10.5% of the 100 pptv h^{-1} external daytime HONO source identified in the plateau's background atmosphere (Wang et al., 2023a). When combined

with the estimated surface nitrate photolysis contribution of ~35 pptv h^{-1} from the same study, these two pathways jointly explain 45.5% of the missing HONO source. These findings highlight that surface processes, particularly soil emissions, play a crucial role in regulating atmospheric HONO and consequently influence the oxidative capacity of the plateau's atmosphere. For NO_x, our estimated soil emissions of 20.3 ± 7.0 Gg N yr^{-1} dwarfs the weak anthropogenic emissions of less than 5 Gg N yr^{-1} reported by Wang et al. (2023a). This establishes soils as the dominant natural NO_x source on the plateau. The high HONO to NO_x (HONO/NO_x) emission ratio, we observed for bare soil (0.49) is consistent with the elevated daytime HONO/NO_x concentration ratio of 0.31 ± 0.06 observed at Nam Co. This observed concentration ratio significantly exceeds the photo-stationary state ratio (0.02–0.05) for internal cycling, which confirms that soil emissions are a primary driver of this chemical disequilibrium. Under intense solar radiation on the Tibetan Plateau, HONO emitted from soils undergoes rapid photolysis to generate OH radicals, while NO_x emissions from soils provide key precursors for tropospheric O_3 production. Continuous warming and wetting of the Tibetan Plateau (Yan et al., 2026) likely further enhance soil Nr emissions, forming positive feedback that strengthens atmospheric oxidation capacity. This climate–chemistry feedback requires accurate representation in Earth system models to support reliable projections of air quality, ecosystem stability, and the lifetime of greenhouse gases over this climatically sensitive region.

Our study further identifies that soil Nr emissions uniquely modulate the regional atmospheric chemical balance by elevating the HONO/NO_x ratio beyond the atmospheric internal cycling equilibrium. Our field-constrained soil NO_x and HONO emission estimates provide key constraints to reduce the underestimation of O_3 production in GEOS-Chem simulations (Wang et al., 2025a) and narrow the gap between modelled and observed atmospheric chemistry over the Third Pole. The distinctiveness of this effect stems from the plateau's extreme environment: intense solar radiation (j_{O^1D} up to 5.5×10^{-5} s^{-1}, double the sea-level value) accelerates HONO photolysis to OH radicals, while the high background O_3 concentrations (Yin et al., 2017) mean soil NO_x emissions sustain O_3 accumulation without significant anthropogenic interference. In contrast to global studies that emphasize the role of soil HONO emissions in particulate matter pollution (Li et al., 2026), our regional observations demonstrate that soil Nr emissions on the Tibetan Plateau directly and strongly regulate atmospheric oxidation capacity and O_3 cycling, with profound cascading effects on regional air quality and climate systems.

4 Conclusions

The Tibetan Plateau's soil Nr emissions exhibit distinct patterns shaped by land-use characteristics and environmental factors. Cropland soils emitted the highest fluxes of HONO, NO, and NO_2, driven by soil pH and inorganic nitrogen content, along with abundant nitrogen-cycling functional genes such as *amoA* and microbial communities dominated by Actinobacteriota and Crenarchaeota. These findings confirm that agricultural soils serve as significant sources of HONO and NO_x due to their unique biogeochemical properties. However, despite higher per-area emissions from croplands, the extensive grassland and bare land areas contributed substantially more to total annual Nr emissions at the regional scale, demonstrating how land-use distribution fundamentally influences nitrogen budgets.

Atmospheric interactions further modulate these emission patterns in complex ways. Exposure to NO_x and O_3 produced divergent responses across ecosystems-forest soils increased emissions, likely through pH elevation and enhanced activity of nitrification genes including *nxrB*, *nirK*, and *nirS* that accelerate NO_3^- and NO_2^- decomposition. Conversely, cropland and grassland soils became emission sinks as altered soil properties, such as accumulated NO_3^- in croplands and reduced NO_2^- in grasslands favored nitrogen retention over release. These contrasting responses highlight the intricate relationships between atmospheric chemistry and soil biogeochemistry mediated by microbial communities.

The regional atmospheric impacts of these emissions prove significant despite modest global contributions. Estimated annual soil emissions reached 7.0 ± 3.4 Gg N yr^{-1} for HONO and 20.3 ± 7.0 Gg N yr^{-1} for NO_x across Tibet. Soil HONO emissions account for approximately 10.5% of the external daytime HONO source identified in the plateau's background atmosphere, modulating the regional atmospheric chemical balance by elevating the HONO/NO_x ratio beyond the atmospheric internal cycling equilibrium. Under the plateau's intense solar radiation, rapid HONO photolysis likely boosted OH· radical production, thereby enhancing atmospheric oxidation capacity. Such processes may exacerbate NO_x and O_3 pollution with cascading effects on regional climate and air quality. These findings underscore soil Nr emissions as crucial components of the Tibetan Plateau's nitrogen cycle and atmospheric chemistry, with implications for understanding climate change impacts and developing mitigation strategies in this ecologically vulnerable region.

Data Availability

The data that supports the findings of this study are available at https://doi.org/10.5281/zenodo.21628446 (Deng et al., 2026).

Author contributions

LLD performed the measurement, data analysis and visualization, and wrote the manuscript. YHC performed the data analysis and visualization and wrote the manuscript. CXY contributed to writing – review & editing. RW performed the measurement and data analysis. RHW and ZHF performed the measurement. HFZ contributed to funding acquisition, methodology, supervision, and writing – review & editing. DMW contributed to conception, funding acquisition, methodology, supervision, and writing – review & editing. LLD and YHC prepared the manuscript with contributions from all co-authors.

Competing interests

The authors declare that they have no conflicts of interest.

Acknowledgements

We acknowledge the staff at the Nam Co Multisphere Observation and Research Station for their assistance in field sampling and data collection. We acknowledge the laboratory and technical support provided by the Key Laboratory of Geographic Information Science (Ministry of Education, East China Normal University), the State Key Joint Laboratory for Environmental Simulation and Pollution Control (Peking University), and the State Key Laboratory of Soil and Sustainable Agriculture (Institute of Soil Sciences, Chinese Academy of Sciences).

Financial support

This study was supported by the National Natural Science Foundation of China (42477328) and the National Key Research and Development Program of China (2023YFC3707401 and 2026YFE0151200).

References

Baker, B.J., De Anda, V., Seitz, K.W., Dombrowski, N., Santoro, A.E. and Lloyd, K.G.: Diversity, ecology and evolution of Archaea. Nature Microbiology 5(7), 887-900, https://dx.doi.org/10.1038/s41564-020-0715-z, 2020.

Bala, G., Devaraju, N., Chaturvedi, R.K., Caldeira, K. and Nemani, R.: Nitrogen deposition: how important is it for global terrestrial carbon uptake? Biogeosciences 10(11), 7147-7160, https://dx.doi.org/10.5194/bg-10-7147-2013, 2013.

Bao, F., Cheng, Y., Kuhn, U., Li, G., Wang, W., Kratz, A.M., Weber, J., Weber, B., Pöschl, U. and Su, H.: Key Role of Equilibrium HONO Concentration over Soil in Quantifying Soil–Atmosphere HONO Fluxes. Environmental Science & Technology 56(4), 2204-2212, https://dx.doi.org/10.1021/acs.est.1c06716, 2022.

Bao, Y., Dolfing, J., Guo, Z., Chen, R., Wu, M., Li, Z., Lin, X. and Feng, Y.: Important ecophysiological roles of non-dominant *Actinobacteria* in plant residue decomposition, especially in less fertile soils. Microbiome 9(1), 84, https://dx.doi.org/10.1186/s40168-021-01032-x, 2021.

Behera, S.N., Sharma, M., Aneja, V.P. and Balasubramanian, R.: Ammonia in the atmosphere: a review on emission sources, atmospheric chemistry and deposition on terrestrial bodies. Environmental Science and Pollution Research 20(11), 8092-8131, https://dx.doi.org/10.1007/s11356-013-2051-9, 2013.

Behrendt, T., Veres, P.R., Ashuri, F., Song, G., Flanz, M., Mamtimin, B., Bruse, M., Williams, J. and Meixner, F.X.: Characterisation of NO production and consumption: new insights by an improved laboratory dynamic chamber technique. Biogeosciences 11(19), 5463-5492, https://dx.doi.org/10.5194/bg-11-5463-2014, 2014.

Berthrong, S.T., Yeager, C.M., Gallegos-Graves, L., Steven, B., Eichorst, S.A., Jackson, R.B. and Kuske, C.R.: Nitrogen Fertilization Has a Stronger Effect on Soil Nitrogen-Fixing Bacterial Communities than Elevated Atmospheric CO_2. Applied and Environmental Microbiology 80(10), 3103-3112, https://dx.doi.org/doi:10.1128/AEM.04034-13, 2014.

Bhattarai, H.R., Virkajärvi, P., Yli-Pirilä, P. and Maljanen, M.: Emissions of atmospherically important nitrous acid (HONO) gas from northern grassland soil increases in the presence of nitrite (NO_2^-). Agriculture, Ecosystems & Environment 256, 194-199, https://dx.doi.org/https://doi.org/10.1016/j.agee.2018.01.017, 2018.

Bhattarai, H.R., Wanek, W., Siljanen, H.M.P., Ronkainen, J.G., Liimatainen, M., Hu, Y., Nykänen, H., Biasi, C. and Maljanen, M.: Denitrification is the major nitrous acid production pathway in boreal agricultural soils. Communications Earth & Environment 2(1), 54, https://dx.doi.org/10.1038/s43247-021-00125-7, 2021.

Bray, C.D., Battye, W.H., Aneja, V.P. and Schlesinger, W.H.: Global emissions of NH_3, NO_x, and N_2O from biomass burning and the impact of climate change. Journal of the Air & Waste Management Association 71(1), 102-114, https://dx.doi.org/10.1080/10962247.2020.1842822, 2021.

Brochier-Armanet, C., Boussau, B., Gribaldo, S. and Forterre, P.: Mesophilic crenarchaeota: proposal for a third archaeal phylum, the Thaumarchaeota. Nature Reviews Microbiology 6(3), 245-252, https://dx.doi.org/10.1038/nrmicro1852, 2008.

Cai, Y., Ding, W. and Xiang, J.: Mechanisms of nitrous oxide and nitric oxide production in soils: A review. Soils 44(5), 712-718, https://dx.doi.org/10.3969/j.issn.0253-9829.2012.05.002, 2012.

Cao, J., Jiao, Y., Che, R., Holden, N.M., Zhang, X., Biswas, A. and Feng, Q.: The effects of grazer exclosure duration on soil microbial communities on the Qinghai-Tibetan Plateau. Science of The Total Environment 839, 156238, https://dx.doi.org/https://doi.org/10.1016/j.scitotenv.2022.156238, 2022.

Cao, J., Wang, H., Holden, N.M., Adamowski, J.F., Biswas, A., Zhang, X. and Feng, Q.: Soil properties and microbiome of annual and perennial cultivated grasslands on the Qinghai–Tibetan Plateau. Land Degradation & Development 32(18), 5306-5321, https://dx.doi.org/https://doi.org/10.1002/ldr.4110, 2021.

Chen, C., Xiao, W. and Chen, H.Y.H.: Mapping global soil acidification under N deposition. Global Change Biology 29(16), 4652-4661, https://dx.doi.org/https://doi.org/10.1111/gcb.16813, 2023.

Chen, H., Ju, P., Zhu, Q., Xu, X., Wu, N., Gao, Y., Feng, X., Tian, J., Niu, S., Zhang, Y., Peng, C. and Wang, Y.: Carbon and nitrogen cycling on the Qinghai–Tibetan Plateau. Nature Reviews Earth & Environment 3(10), 701-716, https://dx.doi.org/10.1038/s43017-022-00344-2, 2022a.

Chen, W., Wang, J., Chen, X., Meng, Z., Xu, R., Duoji, D., Zhang, J., He, J., Wang, Z., Chen, J., Liu, K., Hu, T. and Zhang, Y.: Soil microbial network complexity predicts ecosystem function along elevation gradients on the Tibetan Plateau. Soil Biology and Biochemistry 172, 108766, https://dx.doi.org/https://doi.org/10.1016/j.soilbio.2022.108766, 2022b.

Dang, H., Zhang, X., Sun, J., Li, T., Zhang, Z. and Yang, G.: Diversity and spatial distribution of sediment ammonia-oxidizing crenarchaeota in response to estuarine and environmental gradients in the Changjiang Estuary and East China Sea. Microbiology 154(7), 2084-2095, https://dx.doi.org/https://doi.org/10.1099/mic.0.2007/013581-0, 2008.

Delaria, E.R. and Cohen, R.C.: Measurements of Atmosphere–Biosphere Exchange of Oxidized Nitrogen and Implications for the Chemistry of Atmospheric NO_x. Accounts of Chemical Research 56(13), 1720-1730, https://dx.doi.org/10.1021/acs.accounts.3c00090, 2023.

590 Donaldson, M.A., Bish, D.L. and Raff, J.D.: Soil surface acidity plays a determining role in the atmospheric-terrestrial exchange of nitrous acid. Proceedings of the National Academy of Sciences 111(52), 18472-18477, https://dx.doi.org/doi:10.1073/pnas.1418545112, 2014.

Du, E., Fenn, M.E., De Vries, W. and Ok, Y.S.: Atmospheric nitrogen deposition to global forests: Status, impacts and management options. Environmental Pollution 250, 1044-1048,
595 https://dx.doi.org/https://doi.org/10.1016/j.envpol.2019.04.014, 2019.

Erisman, J.W., Galloway, J., Seitzinger, S., Bleeker, A. and Butterbach-Bahl, K.: Reactive nitrogen in the environment and its effect on climate change. Current Opinion in Environmental Sustainability 3(5), 281-290, https://dx.doi.org/https://doi.org/10.1016/j.cosust.2011.08.012, 2011.

Ermel, M., Behrendt, T., Oswald, R., Derstroff, B., Wu, D., Hohlmann, S., Stönner, C., Pommerening-Röser, A., Könneke,
600 M., Williams, J., Meixner, F.X., Andreae, M.O., Trebs, I. and Sörgel, M.: Hydroxylamine released by nitrifying microorganisms is a precursor for HONO emission from drying soils. Scientific Reports 8(1), 1877, https://dx.doi.org/10.1038/s41598-018-20170-1, 2018.

Fan, M.-Y., Xiang, Y.-K., Zhang, Y.-L., Lin, Y.-C., Cao, F., Jiang, R., Liu, X. and Su, H.: Comparative contributions of primary emission and secondary production of HONO from unfertilized soil in Eastern China. Sustainable Horizons 14,
605 100136, https://dx.doi.org/https://doi.org/10.1016/j.horiz.2025.100136, 2025.

Fierer, N., Lauber, C.L., Ramirez, K.S., Zaneveld, J., Bradford, M.A. and Knight, R.: Comparative metagenomic, phylogenetic and physiological analyses of soil microbial communities across nitrogen gradients. The ISME Journal 6(5), 1007-1017, https://dx.doi.org/10.1038/ismej.2011.159, 2012.

Fowler, D., Coyle, M., Skiba, U., Sutton, M.A., Cape, J.N., Reis, S., Sheppard, L.J., Jenkins, A., Grizzetti, B., Galloway, J.N.,
610 Vitousek, P., Leach, A., Bouwman, A.F., Butterbach-Bahl, K., Dentener, F., Stevenson, D., Amann, M. and Voss, M.: The global nitrogen cycle in the twenty-first century. Philos Trans R Soc Lond B Biol Sci 368(1621), 20130164, https://dx.doi.org/10.1098/rstb.2013.0164, 2013.

Fu, W., Wu, H., Zhao, A.-H., Hao, Z.-P. and Chen, B.-D.: Ecological impacts of nitrogen deposition on terrestrial ecosystems: research progresses and prospects. Chinese Journal of Plant Ecology 44(5), 475-493,
615 https://dx.doi.org/10.17521/cjpe.2019.0163, 2020.

Gao, Y.-h., Ma, X. and Cooper, D.J.: Short-term effect of nitrogen addition on nitric oxide emissions from an alpine meadow in the Tibetan Plateau. Environmental Science and Pollution Research 23, 12474-12479, 2016.

He, J., Li, J. and Zheng, Y.: Thoughts on the microbial diversity-stability relationship in soil ecosystems. Shengwu Duoyangxing 21(4), 411-420, https://dx.doi.org/10.3724/sp.J.1003.2013.10033, 2013.

620 Heil, J., Vereecken, H. and Brüggemann, N.: A review of chemical reactions of nitrification intermediates and their role in nitrogen cycling and nitrogen trace gas formation in soil. European Journal of Soil Science 67(1), 23-39, https://dx.doi.org/https://doi.org/10.1111/ejss.12306, 2016.

Hereid, D.P. and Monson, R.K.: Nitrogen oxide fluxes between corn (*Zea mays* L.) leaves and the atmosphere. Atmospheric Environment 35(5), 975-983, https://dx.doi.org/https://doi.org/10.1016/S1352-2310(00)00342-3, 2001.

Holst, J., Liu, C., Brüggemann, N., Butterbach-Bahl, K., Zheng, X., Wang, Y., Han, S., Yao, Z., Yue, J. and Han, X.: Microbial N Turnover and N-Oxide (N_2O/NO/NO_2) Fluxes in Semi-arid Grassland of Inner Mongolia. Ecosystems 10(4), 623-634, https://dx.doi.org/10.1007/s10021-007-9043-x, 2007.

Hong, S., Li, Z., Tang, M., Li, F., Yao, Y., Yan, Y., He, M., Wang, X., Zeng, H. and Piao, S.: Magnitude, distribution and temporal trend of nitrous oxide emissions from China's natural soils over 1980–2022. Science China Earth Sciences 68(4), 1074-1085, https://dx.doi.org/10.1007/s11430-024-1522-4, 2025.

Jia, Y., Yu, G., Gao, Y., He, N., Wang, Q., Jiao, C. and Zuo, Y.: Global inorganic nitrogen dry deposition inferred from ground- and space-based measurements. Scientific Reports 6(1), 19810, https://dx.doi.org/10.1038/srep19810, 2016.

Johnson, S.S., Hebsgaard, M.B., Christensen, T.R., Mastepanov, M., Nielsen, R., Munch, K., Brand, T., Gilbert, M.T.P., Zuber, M.T., Bunce, M., Rønn, R., Gilichinsky, D., Froese, D. and Willerslev, E.: Ancient bacteria show evidence of DNA repair. Proceedings of the National Academy of Sciences 104(36), 14401-14405, https://dx.doi.org/doi:10.1073/pnas.0706787104, 2007.

Kang, E., Li, Y., Zhang, X., Yan, Z., Wu, H., Li, M., Yan, L., Zhang, K., Wang, J. and Kang, X.: Soil pH and nutrients shape the vertical distribution of microbial communities in an alpine wetland. Science of The Total Environment 774, 145780, https://dx.doi.org/https://doi.org/10.1016/j.scitotenv.2021.145780, 2021.

Kim, M. and Or, D.: Microscale pH variations during drying of soils and desert biocrusts affect HONO and NH_3 emissions. Nature Communications 10(1), 3944, https://dx.doi.org/10.1038/s41467-019-11956-6, 2019.

Kumar, P., Broquet, G., Hauglustaine, D., Beaudor, M., Clarisse, L., Van Damme, M., Coheur, P., Cozic, A., Zheng, B., Revilla Romero, B., Delavois, A. and Ciais, P.: Global atmospheric inversion of the anthropogenic NH_3 emissions over 2019–2022 using the LMDZ-INCA chemistry transport model and the IASI NH_3 observations. Atmos. Chem. Phys. 25(19), 12379-12407, https://dx.doi.org/10.5194/acp-25-12379-2025, 2025.

Leff, J.W., Jones, S.E., Prober, S.M., Barberán, A., Borer, E.T., Firn, J.L., Harpole, W.S., Hobbie, S.E., Hofmockel, K.S., Knops, J.M.H., McCulley, R.L., La Pierre, K., Risch, A.C., Seabloom, E.W., Schütz, M., Steenbock, C., Stevens, C.J. and Fierer, N.: Consistent responses of soil microbial communities to elevated nutrient inputs in grasslands across the globe. Proceedings of the National Academy of Sciences 112(35), 10967-10972, https://dx.doi.org/doi:10.1073/pnas.1508382112, 2015.

Levy-Booth, D.J., Prescott, C.E. and Grayston, S.J.: Microbial functional genes involved in nitrogen fixation, nitrification and denitrification in forest ecosystems. Soil Biology and Biochemistry 75, 11-25, https://dx.doi.org/https://doi.org/10.1016/j.soilbio.2014.03.021, 2014.

Li, M., Mao, J., Chen, S., Bian, J., Bai, Z., Wang, X., Chen, W. and Yu, P.: Significant contribution of lightning NO_x to summertime surface O_3 on the Tibetan Plateau. Science of The Total Environment 829, 154639, https://dx.doi.org/https://doi.org/10.1016/j.scitotenv.2022.154639, 2022.

Li, R., Fan, Q., Shao, Y., Shen, Y., Haider, H., Wu, D., Yao, Y. and Wang, G.: Global Soil Nitrous Acid (HONO) Emission Has Aggravated $PM_{2.5}$ Pollution and Health Risks over the Last Century. Environmental Science & Technology 60(5), 4261-4270, https://dx.doi.org/10.1021/acs.est.5c08207, 2026.

Liang, W., Yang, Z., Luo, J., Tian, H., Bai, Z., Li, D., Li, Q., Zhang, J., Wang, H., Ba, B. and Yang, Y.: Impacts of the atmospheric apparent heat source over the Tibetan Plateau on summertime ozone vertical distributions over Lhasa. Atmospheric and Oceanic Science Letters 14(3), 100047, https://dx.doi.org/https://doi.org/10.1016/j.aosl.2021.100047, 2021.

Lin, F., Liu, C., Hu, X., Fu, Y., Zheng, X., Wang, R., Zhang, W. and Cao, G.: Characterizing nitric oxide emissions from two typical alpine ecosystems. Journal of Environmental Sciences 77, 312-322, https://dx.doi.org/https://doi.org/10.1016/j.jes.2018.08.011, 2019.

Liu, J., Liu, Z., Ma, Z., Yang, S., Yao, D., Zhao, S., Hu, B., Tang, G., Sun, J., Cheng, M., Xu, Z. and Wang, Y.: Detailed budget analysis of HONO in Beijing, China: Implication on atmosphere oxidation capacity in polluted megacity. Atmospheric Environment 244, 117957, https://dx.doi.org/https://doi.org/10.1016/j.atmosenv.2020.117957, 2021.

Liu, M., Huang, X., Song, Y., Tang, J., Cao, J., Zhang, X., Zhang, Q., Wang, S., Xu, T., Kang, L., Cai, X., Zhang, H., Yang, F., Wang, H., Yu, J.Z., Lau, A.K.H., He, L., Huang, X., Duan, L., Ding, A., Xue, L., Gao, J., Liu, B. and Zhu, T.: Ammonia emission control in China would mitigate haze pollution and nitrogen deposition, but worsen acid rain. Proceedings of the National Academy of Sciences 116(16), 7760-7765, https://dx.doi.org/doi:10.1073/pnas.1814880116, 2019.

Liu, X.J., Xu, W., Du, E.Z., Tang, A.H., Zhang, Y., Zhang, Y.Y., Wen, Z., Hao, T.X., Pan, Y.P., Zhang, L., Gu, B.J., Zhao, Y., Shen, J.L., Zhou, F., Gao, Z.L., Feng, Z.Z., Chang, Y.H., Goulding, K., Collett, J.L., Vitousek, P.M. and Zhang, F.S.: Environmental impacts of nitrogen emissions in China and the role of policies in emission reduction. Philosophical Transactions of the Royal Society A: Mathematical, Physical and Engineering Sciences 378(2183), 20190324, https://dx.doi.org/doi:10.1098/rsta.2019.0324, 2020.

Lu, M., Yang, Y., Luo, Y., Fang, C., Zhou, X., Chen, J., Yang, X. and Li, B.: Responses of ecosystem nitrogen cycle to nitrogen addition: a meta-analysis. New Phytologist 189(4), 1040-1050, https://dx.doi.org/https://doi.org/10.1111/j.1469-8137.2010.03563.x, 2011.

Lu, X., Ye, X., Zhou, M., Zhao, Y., Weng, H., Kong, H., Li, K., Gao, M., Zheng, B., Lin, J., Zhou, F., Zhang, Q., Wu, D., Zhang, L. and Zhang, Y.: The underappreciated role of agricultural soil nitrogen oxide emissions in ozone pollution regulation in North China. Nature Communications 12(1), 5021, https://dx.doi.org/10.1038/s41467-021-25147-9, 2021.

Luo, L., Ran, L., Rasool, Q.Z. and Cohan, D.S.: Integrated Modeling of U.S. Agricultural Soil Emissions of Reactive Nitrogen and Associated Impacts on Air Pollution, Health, and Climate. Environmental Science & Technology 56(13), 9265-9276, https://dx.doi.org/10.1021/acs.est.1c08660, 2022.

Lv, P., Sun, S., Zhao, X., Li, Y., Zhao, S., Zhang, J., Hu, Y., Guo, A., Yue, P. and Zuo, X.: Effects of altered precipitation patterns on soil nitrogen transformation in different landscape types during the growing season in northern China. CATENA 222, 106813, https://dx.doi.org/https://doi.org/10.1016/j.catena.2022.106813, 2023.

Lyu, X., Li, K., Guo, H., Morawska, L., Zhou, B., Zeren, Y., Jiang, F., Chen, C., Goldstein, A.H., Xu, X., Wang, T., Lu, X., Zhu, T., Querol, X., Chatani, S., Latif, M.T., Schuch, D., Sinha, V., Kumar, P., Mullins, B., Seguel, R., Shao, M., Xue, L., Wang, N., Chen, J., Gao, J., Chai, F., Simpson, I., Sinha, B. and Blake, D.R.: A synergistic ozone-climate control to address emerging ozone pollution challenges. One Earth 6(8), 964-977, https://dx.doi.org/https://doi.org/10.1016/j.oneear.2023.07.004, 2023.

Ma, L., Jiang, X., Liu, G., Yao, L., Liu, W., Pan, Y. and Zuo, Y.: Environmental Factors and Microbial Diversity and Abundance Jointly Regulate Soil Nitrogen and Carbon Biogeochemical Processes in Tibetan Wetlands. Environmental Science & Technology 54(6), 3267-3277, https://dx.doi.org/10.1021/acs.est.9b06716, 2020.

Ma, R., Yu, K., Xiao, S., Liu, S., Ciais, P. and Zou, J.: Data-driven estimates of fertilizer-induced soil NH_3, NO and N_2O emissions from croplands in China and their climate change impacts. Global Change Biology 28(3), 1008-1022, https://dx.doi.org/https://doi.org/10.1111/gcb.15975, 2022.

Magnani, F., Mencuccini, M., Borghetti, M., Berbigier, P., Berninger, F., Delzon, S., Grelle, A., Hari, P., Jarvis, P.G., Kolari, P., Kowalski, A.S., Lankreijer, H., Law, B.E., Lindroth, A., Loustau, D., Manca, G., Moncrieff, J.B., Rayment, M., Tedeschi, V., Valentini, R. and Grace, J.: The human footprint in the carbon cycle of temperate and boreal forests. Nature 447(7146), 849-851, https://dx.doi.org/10.1038/nature05847, 2007.

Maier, S., Kratz, A.M., Weber, J., Prass, M., Liu, F., Clark, A.T., Abed, R.M.M., Su, H., Cheng, Y., Eickhorst, T., Fiedler, S., Pöschl, U. and Weber, B.: Water-driven microbial nitrogen transformations in biological soil crusts causing atmospheric nitrous acid and nitric oxide emissions. The ISME Journal 16(4), 1012-1024, https://dx.doi.org/10.1038/s41396-021-01127-1, 2022.

Maljanen, M., Yli-Pirilä, P., Hytönen, J., Joutsensaari, J. and Martikainen, P.J.: Acidic northern soils as sources of atmospheric nitrous acid (HONO). Soil Biology and Biochemistry 67, 94-97, https://dx.doi.org/https://doi.org/10.1016/j.soilbio.2013.08.013, 2013.

Mamtimin, B., Meixner, F.X., Behrendt, T., Badawy, M. and Wagner, T.: The contribution of soil biogenic NO and HONO emissions from a managed hyperarid ecosystem to the regional NO_x emissions during growing season. Atmos. Chem. Phys. 16(15), 10175-10194, https://dx.doi.org/10.5194/acp-16-10175-2016, 2016.

McCalley, C.K., Strahm, B.D., Sparks, K.L., Eller, A.S.D. and Sparks, J.P.: The effect of long-term exposure to elevated CO_2 on nitrogen gas emissions from Mojave Desert soils. Journal of Geophysical Research: Biogeosciences 116(G3), G03022, https://dx.doi.org/https://doi.org/10.1029/2011JG001667, 2011.

Medinets, S., Skiba, U., Rennenberg, H. and Butterbach-Bahl, K.: A review of soil NO transformation: Associated processes and possible physiological significance on organisms. Soil Biology and Biochemistry 80, 92-117, https://dx.doi.org/https://doi.org/10.1016/j.soilbio.2014.09.025, 2015.

Meusel, H., Tamm, A., Kuhn, U., Wu, D., Leifke, A.L., Fiedler, S., Ruckteschler, N., Yordanova, P., Lang-Yona, N., Pöhlker, M., Lelieveld, J., Hoffmann, T., Pöschl, U., Su, H., Weber, B. and Cheng, Y.: Emission of nitrous acid from soil and biological

soil crusts represents an important source of HONO in the remote atmosphere in Cyprus. Atmos. Chem. Phys. 18(2), 799-813, https://dx.doi.org/10.5194/acp-18-799-2018, 2018.

Mushinski, R.M., Phillips, R.P., Payne, Z.C., Abney, R.B., Jo, I., Fei, S., Pusede, S.E., White, J.R., Rusch, D.B. and Raff, J.D.: Microbial mechanisms and ecosystem flux estimation for aerobic NO_y emissions from deciduous forest soils. Proceedings of the National Academy of Sciences 116(6), 2138-2145, https://dx.doi.org/doi:10.1073/pnas.1814632116, 2019.

Ning, Q., Gu, Q., Shen, J., Lv, X., Yang, J., Zhang, X., He, J., Huang, J., Wang, H., Xu, Z. and Han, X.: Effects of nitrogen deposition rates and frequencies on the abundance of soil nitrogen-related functional genes in temperate grassland of northern China. Journal of Soils and Sediments 15(3), 694-704, https://dx.doi.org/10.1007/s11368-015-1061-2, 2015.

Oswald, R., Behrendt, T., Ermel, M., Wu, D., Su, H., Cheng, Y., Breuninger, C., Moravek, A., Mougin, E., Delon, C., Loubet, B., Pommerening-Röser, A., Sörgel, M., Pöschl, U., Hoffmann, T., Andreae, M.O., Meixner, F.X. and Trebs, I.: HONO Emissions from Soil Bacteria as a Major Source of Atmospheric Reactive Nitrogen. Science 341(6151), 1233-1235, https://dx.doi.org/doi:10.1126/science.1242266, 2013.

Pilegaard, K.: Processes regulating nitric oxide emissions from soils. Philosophical Transactions of the Royal Society B: Biological Sciences 368(1621), 20130126, https://dx.doi.org/doi:10.1098/rstb.2013.0126, 2013.

Ren, C., Huang, X., Wang, Y., Zhang, L., Zhou, X., Sun, W., Zhang, H., Liu, T., Ding, A. and Wang, T.: Enhanced Soil Emissions of Reactive Nitrogen Gases by Fertilization and Their Impacts on Secondary Air Pollution in Eastern China. Environmental Science & Technology 59(10), 5119-5130, https://dx.doi.org/10.1021/acs.est.4c12324, 2025.

Scharko, N.K., Schütte, U.M.E., Berke, A.E., Banina, L., Peel, H.R., Donaldson, M.A., Hemmerich, C., White, J.R. and Raff, J.D.: Combined Flux Chamber and Genomics Approach Links Nitrous Acid Emissions to Ammonia Oxidizing Bacteria and Archaea in Urban and Agricultural Soil. Environmental Science & Technology 49(23), 13825-13834, https://dx.doi.org/10.1021/acs.est.5b00838, 2015.

Škerlak, B., Sprenger, M. and Wernli, H.: A global climatology of stratosphere–troposphere exchange using the ERA-Interim data set from 1979 to 2011. Atmos. Chem. Phys. 14(2), 913-937, https://dx.doi.org/10.5194/acp-14-913-2014, 2014.

Slessarev, E.W., Lin, Y., Bingham, N.L., Johnson, J.E., Dai, Y., Schimel, J.P. and Chadwick, O.A.: Water balance creates a threshold in soil pH at the global scale. Nature 540(7634), 567-569, https://dx.doi.org/10.1038/nature20139, 2016.

Song, S., Zhang, C., Gao, Y., Zhu, X., Wang, R., Wang, M., Zheng, Y., Hou, L., Liu, M. and Wu, D.: Responses of wetland soil bacterial community and edaphic factors to two-year experimental warming and *Spartina alterniflora* invasion in Chongming Island. Journal of Cleaner Production 250, 119502, https://dx.doi.org/https://doi.org/10.1016/j.jclepro.2019.119502, 2020.

Song, Y., Wu, D., Dörsch, P., Yue, L., Deng, L., Liao, C., Sha, Z., Dong, W. and Yu, Y.: Adaptation of NO_2^- Extraction Methods to Different Agricultural Soils: Fine-Tuning Based on Existing Techniques. Agronomy 14(2), 331, 2024.

Song, Y., Wu, D., Ju, X., Dörsch, P., Wang, M., Wang, R., Song, X., Deng, L., Wang, R., Gao, Z., Haider, H., Hou, L., Liu, M. and Yu, Y.: Nitrite stimulates HONO and NO_x but not N_2O emissions in Chinese agricultural soils during nitrification. Science of The Total Environment 902, 166451, https://dx.doi.org/https://doi.org/10.1016/j.scitotenv.2023.166451, 2023.

Sörgel, M., Trebs, I., Wu, D. and Held, A.: A comparison of measured HONO uptake and release with calculated source strengths in a heterogeneous forest environment. Atmos. Chem. Phys. 15(16), 9237-9251, https://dx.doi.org/10.5194/acp-15-9237-2015, 2015.

Su, H., Cheng, Y., Oswald, R., Behrendt, T., Trebs, I., Meixner, F.X., Andreae, M.O., Cheng, P., Zhang, Y. and Pöschl, U.: Soil Nitrite as a Source of Atmospheric HONO and OH Radicals. Science 333(6049), 1616-1618, https://dx.doi.org/doi:10.1126/science.1207687, 2011.

Su, H., Cheng, Y. and Pöschl, U.: The Exchange of Soil Nitrite and Atmospheric HONO: A Missing Process in the Nitrogen Cycle and Atmospheric Chemistry. Journal (Issue), 93-99, 2013.

Sutton, M.A., Reis, S. and Bahl, K.B.: Reactive nitrogen in agroecosystems: Integration with greenhouse gas interactions. Agriculture, Ecosystems & Environment 133(3), 135-138, https://dx.doi.org/https://doi.org/10.1016/j.agee.2009.06.008, 2009.

Swarnalakshmi, K., Senthilkumar, M. and Ramakrishnan, B.: Endophytic Actinobacteria: Nitrogen Fixation, Phytohormone Production, and Antibiosis, Springer Singapore, Singapore. https://doi.org/10.1007/978-981-10-0707-1_8, 2016.

Tang, K., Qin, M., Duan, J., Fang, W., Meng, F., Liang, S., Xie, P., Liu, J., Liu, W., Xue, C. and Mu, Y.: A dual dynamic chamber system based on IBBCEAS for measuring fluxes of nitrous acid in agricultural fields in the North China Plain. Atmospheric Environment 196, 10-19, https://dx.doi.org/https://doi.org/10.1016/j.atmosenv.2018.09.059, 2019.

Tang, L., Hu, M., Shang, D., Fang, X., Mao, J., Xu, W., Zhou, J., Zhao, W., Wang, Y., Zhang, C., Zhang, Y., Hu, J., Zeng, L., Ye, C., Guo, S. and Wu, Z.: High frequency of new particle formation events driven by summer monsoon in the central Tibetan Plateau, China. Atmos. Chem. Phys. 23(7), 4343-4359, https://dx.doi.org/10.5194/acp-23-4343-2023, 2023.

Tian, X., Yin, Y., He, K., Qiu, R., Cong, J., Wang, Z., Yu, H., Chen, Z., Chu, Y., Ying, H. and Cui, Z.: Data-driven estimation of nitric oxide emissions from global soils based on dominant vegetation covers. Global Change Biology 29(20), 5955-5967, https://dx.doi.org/https://doi.org/10.1111/gcb.16864, 2023.

Treseder, K.K.: Nitrogen additions and microbial biomass: a meta-analysis of ecosystem studies. Ecology Letters 11(10), 1111-1120, https://dx.doi.org/https://doi.org/10.1111/j.1461-0248.2008.01230.x, 2008.

VandenBoer, T.C., Young, C.J., Talukdar, R.K., Markovic, M.Z., Brown, S.S., Roberts, J.M. and Murphy, J.G.: Nocturnal loss and daytime source of nitrous acid through reactive uptake and displacement. Nature Geoscience 8(1), 55-60, https://dx.doi.org/10.1038/ngeo2298, 2015.

Wang, C., Liu, D. and Bai, E.: Decreasing soil microbial diversity is associated with decreasing microbial biomass under nitrogen addition. Soil Biology and Biochemistry 120, 126-133, https://dx.doi.org/https://doi.org/10.1016/j.soilbio.2018.02.003, 2018.

Wang, J., Wang, H., Zhang, C., Wang, Y., Zhang, Y., Zhou, J., Xu, W., Whalley, L.K., Dyson, J.E., Slater, E.J., Xing, C., Chi, S., Wang, Y., Wang, L., Yu, X., Zeng, L., Lin, W., Zhao, W., Heard, D.E., Song, S. and Ye, C.: Ozone Production Underestimation Over the Tibetan Plateau: The Role of NO_x and OVOCs Modeling Uncertainties. Journal of Geophysical Research: Atmospheres 130(10), e2025JD043321, https://dx.doi.org/https://doi.org/10.1029/2025JD043321, 2025a.

Wang, J., Zhang, Y., Zhang, C., Wang, Y., Zhou, J., Whalley, L.K., Slater, E.J., Dyson, J.E., Xu, W., Cheng, P., Han, B., Wang, L., Yu, X., Wang, Y., Woodward-Massey, R., Lin, W., Zhao, W., Zeng, L., Ma, Z., Heard, D.E. and Ye, C.: Validating HONO as an Intermediate Tracer of the External Cycling of Reactive Nitrogen in the Background Atmosphere. Environmental Science & Technology 57(13), 5474-5484, https://dx.doi.org/10.1021/acs.est.2c06731, 2023a.

Wang, Y., Liu, Y., Xia, L., Akiyama, H., Chen, X., Chen, J., Fang, Y., Vancov, T., Li, Y., Yao, Y., Wu, D., Yu, B., Chang, S.X. and Cai, Y.: Accounting for differences between crops and regions reduces estimates of nitrate leaching from nitrogen-fertilized soils. Communications Earth & Environment 6(1), 29, https://dx.doi.org/10.1038/s43247-025-02001-0, 2025b.

Wang, Y., Sheng, H.-F., He, Y., Wu, J.-Y., Jiang, Y.-X., Tam, N.F.-Y. and Zhou, H.-W.: Comparison of the Levels of Bacterial Diversity in Freshwater, Intertidal Wetland, and Marine Sediments by Using Millions of Illumina Tags. Applied and Environmental Microbiology 78(23), 8264-8271, https://dx.doi.org/doi:10.1128/AEM.01821-12, 2012.

Wang, Z., Huang, L. and Shao, M.a.: Spatial variations and influencing factors of soil organic carbon under different land use types in the alpine region of Qinghai-Tibet Plateau. CATENA 220, 106706, https://dx.doi.org/https://doi.org/10.1016/j.catena.2022.106706, 2023b.

Weber, B., Wu, D., Tamm, A., Ruckteschler, N., Rodríguez-Caballero, E., Steinkamp, J., Meusel, H., Elbert, W., Behrendt, T., Sörgel, M., Cheng, Y., Crutzen, P.J., Su, H. and Pöschl, U.: Biological soil crusts accelerate the nitrogen cycle through large NO and HONO emissions in drylands. Proceedings of the National Academy of Sciences 112(50), 15384-15389, https://dx.doi.org/doi:10.1073/pnas.1515818112, 2015.

Wu, D., Deng, L., Liu, Y., Xi, D., Zou, H., Wang, R., Sha, Z., Pan, Y., Hou, L. and Liu, M.: Comparisons of the effects of different drying methods on soil nitrogen fractions: Insights into emissions of reactive nitrogen gases (HONO and NO). Atmospheric and Oceanic Science Letters 13(3), 224-231, https://dx.doi.org/10.1080/16742834.2020.1733388, 2020.

Wu, D., Deng, L., Sun, Y., Wang, R., Zhang, L., Wang, R., Song, Y., Gao, Z., Haider, H., Wang, Y., Hou, L. and Liu, M.: Climate warming, but not *Spartina alterniflora* invasion, enhances wetland soil HONO and NO_x emissions. Science of The Total Environment 823, 153710, https://dx.doi.org/https://doi.org/10.1016/j.scitotenv.2022.153710, 2022a.

Wu, D., Horn, M.A., Behrendt, T., Müller, S., Li, J., Cole, J.A., Xie, B., Ju, X., Li, G., Ermel, M., Oswald, R., Fröhlich-Nowoisky, J., Hoor, P., Hu, C., Liu, M., Andreae, M.O., Pöschl, U., Cheng, Y., Su, H., Trebs, I., Weber, B. and Sörgel, M.: Soil HONO emissions at high moisture content are driven by microbial nitrate reduction to nitrite: tackling the HONO puzzle. The ISME Journal 13(7), 1688-1699, https://dx.doi.org/10.1038/s41396-019-0379-y, 2019.

Wu, D., Zhang, J., Wang, M., An, J., Wang, R., Haider, H., Xu-Ri, Huang, Y., Zhang, Q., Zhou, F., Tian, H., Zhang, X., Deng, L., Pan, Y., Chen, X., Yu, Y., Hu, C., Wang, R., Song, Y., Gao, Z., Wang, Y., Hou, L. and Liu, M.: Global and Regional Patterns of Soil Nitrous Acid Emissions and Their Acceleration of Rural Photochemical Reactions. Journal of Geophysical Research: Atmospheres 127(6), e2021JD036379, https://dx.doi.org/https://doi.org/10.1029/2021JD036379, 2022b.

Wu, F., Zhao, Y., Zhang, S., Liu, K. and Han, T.: Analysis and Prospect of the Causes and Prevention Measures of Soil Acidification in Farmland. Environmental Science 47(1), 531-542, https://dx.doi.org/10.13227/j.hjkx.202412155, 2026.

Xu, W., Bian, Y., Lin, W., Zhang, Y., Wang, Y., Ma, Z., Zhang, X., Zhang, G., Ye, C. and Xu, X.: O_3 and PAN in southern Tibetan Plateau determined by distinct physical and chemical processes. Atmos. Chem. Phys. 23(13), 7635-7652, https://dx.doi.org/10.5194/acp-23-7635-2023, 2023.

Xu, X., Zhang, H., Lin, W., Wang, Y., Xu, W. and Jia, S.: First simultaneous measurements of peroxyacetyl nitrate (PAN) and ozone at Nam Co in the central Tibetan Plateau: impacts from the PBL evolution and transport processes. Atmos. Chem. Phys. 18(7), 5199-5217, https://dx.doi.org/10.5194/acp-18-5199-2018, 2018.

Xue, C., Ye, C., Lu, K., Liu, P., Zhang, C., Su, H., Bao, F., Cheng, Y., Wang, W., Liu, Y., Catoire, V.r., Ma, Z., Zhao, X., Song, Y., Ma, X., McGillen, M.R., Mellouki, A., Mu, Y. and Zhang, Y.: Reducing Soil-Emitted Nitrous Acid as a Feasible Strategy for Tackling Ozone Pollution. Environmental Science & Technology 58(21), 9227-9235, https://dx.doi.org/10.1021/acs.est.4c01070, 2024.

Xue, C., Ye, C., Zhang, C., Catoire, V., Liu, P., Gu, R., Zhang, J., Ma, Z., Zhao, X., Zhang, W., Ren, Y., Krysztofiak, G., Tong, S., Xue, L., An, J., Ge, M., Mellouki, A. and Mu, Y.: Evidence for Strong HONO Emission from Fertilized Agricultural Fields and its Remarkable Impact on Regional O_3 Pollution in the Summer North China Plain. ACS Earth and Space Chemistry 5(2), 340-347, https://dx.doi.org/10.1021/acsearthspacechem.0c00314, 2021.

Xue, C., Ye, C., Zhang, Y., Ma, Z., Liu, P., Zhang, C., Zhao, X., Liu, J. and Mu, Y.: Development and application of a twin open-top chambers method to measure soil HONO emission in the North China Plain. Science of The Total Environment 659, 621-631, https://dx.doi.org/https://doi.org/10.1016/j.scitotenv.2018.12.245, 2019.

Yan, X., Shi, G., Li, R., Li, Y., Chai, J., Xu, B., Wang, L., Huang, Y., Li, Z. and Hastings, M.: Declining $\Delta^{17}O$ of nitrate in the northeastern Tibetan Plateau reveals changing atmospheric oxidative capacity. Communications Earth & Environment 7(1), 231, https://dx.doi.org/10.1038/s43247-026-03266-9, 2026.

Yang, F., Zhang, Z., Barberán, A., Yang, Y., Hu, S. and Guo, H.: Nitrogen-induced acidification plays a vital role driving ecosystem functions: Insights from a 6-year nitrogen enrichment experiment in a Tibetan alpine meadow. Soil Biology and Biochemistry 153, 108107, https://dx.doi.org/https://doi.org/10.1016/j.soilbio.2020.108107, 2021.

Yang, J. and Huang, X.: The 30 m annual land cover datasets and its dynamics in China from 1985 to 2024. Earth System Science Data 13(1), 3907-3925, https://dx.doi.org/10.5281/zenodo.15853565, 2025.

Yang, Y., Chen, Q., Yu, W. and Shi, Z.: Estimating soil bacterial abundance and diversity in the Southeast Qinghai-Tibet Plateau. Geoderma 416, 115807, https://dx.doi.org/https://doi.org/10.1016/j.geoderma.2022.115807, 2022.

Yao, Z., Ma, L., Zhang, H., Zheng, X., Wang, K., Zhu, B., Wang, R., Wang, Y., Zhang, W., Liu, C. and Butterbach-Bahl, K.: Characteristics of annual greenhouse gas flux and NO release from alpine meadow and forest on the eastern Tibetan Plateau. Agricultural and Forest Meteorology 272-273, 166-175, https://dx.doi.org/https://doi.org/10.1016/j.agrformet.2019.04.007, 2019.

Yin, X., Kang, S., de Foy, B., Cong, Z., Luo, J., Zhang, L., Ma, Y., Zhang, G., Rupakheti, D. and Zhang, Q.: Surface ozone at Nam Co in the inland Tibetan Plateau: variation, synthesis comparison and regional representativeness. Atmos. Chem. Phys. 17(18), 11293-11311, https://dx.doi.org/10.5194/acp-17-11293-2017, 2017.

Yu, G., Jia, Y., He, N., Zhu, J., Chen, Z., Wang, Q., Piao, S., Liu, X., He, H., Guo, X., Wen, Z., Li, P., Ding, G. and Goulding, K.: Stabilization of atmospheric nitrogen deposition in China over the past decade. Nature Geoscience 12(6), 424-429, https://dx.doi.org/10.1038/s41561-019-0352-4, 2019.

Zhang, H., Yao, Z., Wang, K., Zheng, X., Ma, L., Wang, R., Liu, C., Zhang, W., Zhu, B., Tang, X., Hu, Z. and Han, S.: Annual N_2O emissions from conventionally grazed typical alpine grass meadows in the eastern Qinghai–Tibetan Plateau. Science of The Total Environment 625, 885-899, https://dx.doi.org/https://doi.org/10.1016/j.scitotenv.2017.12.216, 2018a.

Zhang, T.a., Chen, H.Y.H. and Ruan, H.: Global negative effects of nitrogen deposition on soil microbes. The ISME Journal 12(7), 1817-1825, https://dx.doi.org/10.1038/s41396-018-0096-y, 2018b.

Zhang, X.F., Zhao, L., Xu, S.J., Jr, Liu, Y.Z., Liu, H.Y. and Cheng, G.D.: Soil moisture effect on bacterial and fungal community in Beilu River (Tibetan Plateau) permafrost soils with different vegetation types. Journal of Applied Microbiology 114(4), 1054-1065, https://dx.doi.org/10.1111/jam.12106, 2013.

Zhu, H., Chen, Y., Zhao, Y., Zhang, L., Zhang, X., Zheng, B., Liu, L., Pan, Y., Xu, W. and Liu, X.: The Response of Nitrogen Deposition in China to Recent and Future Changes in Anthropogenic Emissions. Journal of Geophysical Research: Atmospheres 127(23), e2022JD037437, https://dx.doi.org/https://doi.org/10.1029/2022JD037437, 2022.

Zhu, X., Shen, J., Li, Y., Liu, X., Xu, W., Zhou, F., Wang, J., Reis, S. and Wu, J.: Nitrogen emission and deposition budget in an agricultural catchment in subtropical central China. Environmental Pollution 289, 117870, https://dx.doi.org/https://doi.org/10.1016/j.envpol.2021.117870, 2021.

Zou, L., Bai, Y.-p., Huang, J., Xiao, D.-r. and Yang, G.: Soil pH and dissolved organic carbon shape microbial communities in wetlands with two different vegetation types in Changdu area, Tibet. Journal of Mountain Science 20(3), 750-764, https://dx.doi.org/10.1007/s11629-022-7753-3, 2023.